CLM - P 539

CLM - P 539

UKAEA

Preprint

A THEORETICAL AND EXPERIMENTAL STUDY OF SPACE CHARGE IN INTENSE ION BEAMS

A J T HOLMES

CULHAM LABORATORY
Abingdon Oxfordshire

1978

CLM-P 539

A THEORETICAL AND EXPERIMENTAL STUDY OF SPACE CHARGE IN INTENSE ION BEAMS

A J T Holmes
Culham Laboratory, Abingdon, Oxon. OX14 3DB, UK.
(Euratom/UKAEA Fusion Association)

A B S T R A C T

The highly collimated beams of energetic neutral atoms used in controlled thermonuclear fusion research (CTR) require the virtual elimination of space charge forces in the primary ion beam in order to minimise the angular divergence. A model is presented which describes the behaviour of an intense ion beam passing through a gas cell. This theory is used to derive the space charge field produced by such a beam and shows how its effect can be minimised.

This model agrees well with experimental measurements and enables emittance dominated beams of very high brightness to be obtained which could find applications in fields other than CTR.

(Submitted for publication in Physical Review)

May 1978

1. INTRODUCTION

The injection of beams of energetic neutral atoms is one of the major methods of auxiliary heating presently in use in the field of controlled thermonuclear research (Cordey [1,2] and Kulsrad and Jassby [3]). These beams are formed by electron capture of a positive ion beam passing through a gas cell. In order to maximise the power transfer from the ion source to the fusion plasma, and also to minimise the flux of thermal gas, the ion beam and therefore the resulting neutral beam, should be highly collimated.

Part of the neutral beam injection development programme at the Culham Laboratory has been specifically aimed towards elucidating the fundamental limits to the divergence of ion beams passing through gas at low pressure. It has been found that residual space charge expansion of a nominally space charge neutralized beam was one of the major processes responsible for divergence angles of the order of 1^{o} observed in previous work. A model is presented below which describes the processes involved in the space charge neutralization of ion beams and, using the predictions of this model, ion beams have been generated in which the divergence due to residual space charge expansion is insignificant compared with that due to the finite temperature of the beam ions.

Although developed for fusion research, these low divergence beams ($\sim 0.2^{o}$) which have a normalized brightness of 3×10^{12} mA cm^{-2} ster^{-1} may find other applications.

2. PHYSICAL PROCESSES

The model considers a non-relativistic ion beam, remote from any conducting walls, passing through a gas at low pressure. Electrons, produced by ionization, are trapped within the beam by its own space charge resulting in a decrease of the effective beam perveance, and hence space charge expansion, to a value which is considerably less than that of the unneutralized beam. The energy and particle balance of this system are explored in some detail as functions of the various physical parameters of the primary beam and in

particular as a function of the ambient gas pressure. The use of Poisson's equation enables a self-consistent description of the beam plasma to be made, including the radial dependence of the potential and particle densities within the beam. It is the radial electric field of the beam plasma which is responsible for the space charge expansion of the beam.

In previous theoretical treatments of space charge neutralization of ion beams, either the continuity or the energy balance equation has been neglected or Poisson's equation has been replaced by the plasma neutrality equation. In the model described by Gabovich et al. [4], electron continuity is neglected and plasma neutrality for a uniform density beam is assumed, thus losing all spatial information. An alternative model developed by Hamilton [5] neglects the effects of the slow ions formed by ionization and also uses the plasma neutrality condition. The neutralization of electron beams, which is very similar, is discussed by Dunn and Self [6] who have solved Poisson's equation by giving an analytic spatial distribution for the electrons and slow ions in a uniform beam but they do not consider the energy balance of the plasma, which controls the electron temperature. Green [7] has extended this model of Dunn and Self to cover ion beams but does not consider energy balance.

The model presented here uses the continuity equation to describe the slow ion and electron densities and the electron temperature is determined by considering the overall energy balance of the beam plasma system. The potential we can then be found by using Poisson's equation, thus completing the description of the beam plasma. Unfortunately these equations are complex and involve four nonlinear differential equations which would require very sophisticated numerical techniques for solution. A slightly simpler approach is adopted here which creates an approximate intermediate solution for the potential which allows the four differential equations to be reduced to a single non-linear equation which still requires a numerical solution, but is considerably simpler to obtain. This new solution replaces the intermediate solution and also provides a comparison to ensure that the intermediate solution is a

good approximation. An even simpler technique of solution is also presented which replaces Poisson's equation by plasma neutrality and discards the spatial distribution functions. This method obtains approximate analytic expressions describing the axial potential and charge densities as functions of the main beam parameters and is useful in understanding the general scaling laws of the beam plasma.

The continuity equation is applied separately to each species of particle. The slow ion flux is determined by an equilibrium between the rate of creation by ionization and charge exchanging collisions and the rate of expulsion by the radial electric field. The electrons, however, are trapped by this electric field and can only escape by diffusion in velocity space via electron-electron collisions until they reach the tail of the Maxwellian distribution and escape.

The electrons formed by ionization extract energy from the primary ion beam by coulomb collisions. The electron heating by the beam is controlled by the detailed shape of the electron distribution at low velocities which is modified by the presence of newly created electrons. The Fokker-Planck equation is used to determine the electron distribution function which is treated as a perturbed Maxwellian distribution. The heated electrons control the magnitude of the potential well and hence determine the energy removed by the escaping slow ions as they are accelerated radially outwards. This energy is equal to the average binding energy of electrons trapped in the well and if these electrons are to escape, they must absorb an equivalent energy from the primary ion beam.

Green [7] has pointed out that the slow ions formed by charge exchange are not involved in the above energy balance. The energy for this process comes directly from the beam ions which are all decelerated by the space charge potential shortly after they have left the emitter which is assumed to be at the wall potential. In the absence of charge exchange, the beam ions are re-accelerated to their full energy when they leave the space

charge well at the distant target (also at the wall potential) and there is no net energy transfer. However, if a beam ion is converted to a fast neutral within the well, it cannot be re-accelerated and the energy lost by the beam ion entering the space charge well is removed by the resulting slow ion when it is expelled radially. Hence this energy transfer is independent of the beam parameters and does not affect the electron temperature.

3. THE CONTINUITY EQUATION

The densities of the slow ions and electrons can be derived from the solution of the continuity equation in terms of the other plasma parameters. The general form of the equation is:

$$\partial n_j/\partial t + \nabla.\underline{F}_j = 0 \qquad \ldots (1)$$

where $\partial n_j/\partial t$ is the creation (or loss) rate of particle j and F_j is the particle flux. This flux describes the motion of each species which in the case of slow ions is free fall under the influence of the electric field. The electrons, however, are assumed to be borne with essentially zero velocity and hence they are electrostatically contained by the fast ion space charge. In this case the escaping electron flux is governed by their diffusion in velocity space. These fluxes and their effect on the particle densities are discussed in the next section.

It is assumed that the beam ions alone are responsible for the creation of slow ions and electrons. The secondary electron energy distribution lacks a high energy tail (see Section 3.2 and Fig.1) and hence the production rate of ion-electron pairs by these electrons is very much less than that of the beam for the experimental situation discussed here (ie. $10^{-6} < p < 10^{-2}$ torr).

3.1 Ions

It is now appropriate to use the integral form of equation 1, obtained by the use of Green's theorem, which gives:

$$\int_V \frac{\partial n_j}{\partial t}\, dV = \int_S \underline{F}_j.\underline{dS}$$

As the beam has cylindrical symmetry, the ion flux is purely radial and they can only escape at infinity, there being no sinks for ions at finite radius (the conducting walls are assumed to be at infinity). Hence for a creation rate dn_i/dt in an element of volume $2\pi\rho d\rho dz$ and where these ions move to a surface at r, the above equation transforms to:-

$$\frac{\partial n_i}{\partial t} \cdot 2\pi\rho d\rho dz = 2\pi\, rdz\, F_i$$

$$= 2\pi\, rdz\, v(\rho,r).dn_i(r)$$

where $v(\rho,r)$ is the velocity at r of those ions produced at ρ and $dn_i(r)$ is the contribution to the density of the ions at r. Integration gives:

$$n_i(r) = \frac{1}{r}\int_o^r \frac{\partial n_i}{\partial t}\frac{\rho d\rho}{v(\rho,r)} \cdot \qquad \ldots (2)$$

The slow ions are created by ionization and charge exchange and move freely under the influence of the electric field. (Scattering is unimportant as the time they spend within the beam is typically the order of one microsecond and is much less than the coulomb interaction time for pressures less than 0.1 torr). Hence

$$n_i(r) = \frac{1}{r}\int_o^r \frac{n_b\, \sigma v_b\, n\, \rho d\rho}{(2e/m_i)^{\frac{1}{2}}(-\phi(r)+\phi(\rho))^{\frac{1}{2}}} \qquad \ldots (3)$$

where n_b is the beam density at ρ, v_b is the beam velocity, n is the gas density and σ is the sum of the ionization and charge exchange cross-sections.

It is shown in Appendix I that the only finite solution for n_i at small values of r is:

$$\lim_{r\to 0} n_i(r) = n_{io} = n_{bo} r_o \sigma n\, v_b m_i^{\frac{1}{2}}/(2e\phi_o)^{\frac{1}{2}} \qquad \ldots (4)$$

where ϕ_o is defined as the first coefficient of the series

$$-\phi(r) = \phi_o \frac{r^2}{r_o^2} + \phi_1 \frac{r^3}{r_o^3} + \text{----}$$

Hence the potential well has a parabolic form close to the beam axis. At larger radii where $n_b \neq n_{bo}$, the potential need no longer remain parabolic and n_i can be found by numerical integration of equation (2).

3.2 Electrons

Low energy electrons created within the beam are trapped by the space charge of the fast ions. To the lowest order, electron-electron collisions lead to the development of a Maxwellian distribution, characterised by a temperature T(eV); diffusion in velocity space allows the electrons which would have populated the high energy tail of the distribution to escape. Hence the electron particle balance is governed by the rate of electron production by ionization and the rate of escape which is determined by the depth of the potential well, and the electron temperature and density. The corresponding energy balance required to maintain this temperature is discussed in Section 4.

Clearly the lifetime of an individual electron depends upon its position in the well; an electron created near the beam axis, and therefore at the bottom of the well, must diffuse much further in velocity space prior to being able to escape than one created near the beam edge where the well is relatively shallow. The electron density in velocity space can be obtained in terms of the source function, electron temperature and potential distribution. The electron density in real space can then be found by recalling that the coordinates of real and velocity space are coupled via the potential well.

Spitzer [8] has shown that the time for a sub-group of electrons to increase their velocity dispersion by an amount v in the directions perpendicular and parallel to their original motion is:

$$\tau_\perp = v^2/\langle(\omega_\perp)^2\rangle \ , \ \tau_{||} = v^2/\langle(\omega_{||})^2\rangle$$

where $\langle(\omega_{||})^2\rangle$ and $\langle(\omega_\perp)^2\rangle$ are the dispersion coefficients in these directions. For a Maxwellian electron distribution of density $n_e(r)$, and using Spitzer's notation, these are:

$$\langle(\omega_{\parallel})^2\rangle = \frac{e^4 n_e \ell n \Lambda}{2\pi\varepsilon_o{}^2 m_e{}^2} \cdot \frac{G(\ell_f\omega)}{\omega} = A_d \frac{G(\ell_f\omega)}{\omega}$$

$$\langle(\omega_{\perp})^2\rangle = \frac{A_d}{\omega} (\mathrm{erf}(\ell_f\omega) - G(\ell_f\omega)$$

where ω is the electron test particle velocity. If, as is the case here, the electron test particles in the sub-group are identical with the main distribution then $\omega\ell_f$ equals $\sqrt{1.5}$.

Since the initial velocities in the sub-group are randomly orientated, neither the perpendicular or parallel directions have any special significance and the two diffusion times may be combined to give a net time:

$$\tau = (1/\tau_{\perp} + 1/\tau_{\parallel})^{-1} = v^2(\langle(\omega_{\perp})^2\rangle + \langle(\omega_{\parallel})^2\rangle)$$

$$= v^2\omega/A_d \ \mathrm{erf}(\sqrt{1.5})$$

The velocity dispersion coefficient may be considered as a diffusion coefficient in velocity space with a magnitude:

$$D_v = \frac{\mathrm{erf}(\sqrt{1.5})A_d}{\omega} = \frac{0.97\ e^4 n_e \ell n \Lambda}{2\pi\varepsilon_o{}^2 m_e{}^2 \omega}$$

$$= C.n_e$$

This diffusion coefficient scales differently from the neutral gas diffusion coefficient as it is proportional to the particle density.

The potential well which surrounds the beam relates the velocity of the electrons to their radius of oscillation in the well. Hence diffusion in velocity space is equivalent to radial diffusion in real space and the source distribution function in real space causes the electrons to have an analogous source function in velocity space. As it has been assumed that the velocity distribution is Maxwellian throughout the potential well, it is not necessary to use the full distribution function, f, for the electrons. Instead, a simplified function, n_v, which describes the number of electrons whose velocity lies in the range v to v + dv relative to a given origin can be used. This velocity can be directly related to the binding potential and containment time since the electrons spend most of their time

at the turning points of the oscillation and they also conserve their random kinetic energy.

The primary ion beam is assumed to be axially and azimuthally uniform with no spatial diffusion in these directions, hence

$$n_v = n_e \cdot \left| \frac{2\pi r dr}{2\pi v_r dv_r} \right|$$

where v_r represents the velocity increment to escape. The diffusion equation can be represented by:

$$\nabla \cdot (D_v \nabla n_v) = - \frac{dn_v}{dt}$$

which in cylindrical geometry becomes:

$$\frac{1}{v_r} \frac{d}{dv_r} \left(v_r D_r \frac{dn_v}{dv_r} \right) = - n n_b \sigma_i v_b \cdot \frac{2\pi r dr}{2\pi v_r dv_r} \qquad \ldots (5)$$

Before further progress can be made the beam profile must be known. The beam profile is assumed, a priori, to have a gaussian shape so that:

$$n_b = n_{bo} \exp(- r^2/r_o^2) \qquad \ldots (6)$$

Hence the first integration of equation 5 can be made giving

$$v_r D_v \frac{dn_v}{dv_r} = \frac{n n_{bo} \sigma_i v_b r_o^2}{2} \cdot \exp(- r^2/r_o^2) + A \qquad \ldots (7)$$

In order to integrate further, the transform relation between v_r and r must be determined.

There are two natural co-ordinate systems in velocity space, namely one where the velocity is related to the potential energy associated with the radius of oscillation so that v = 0 when r = 0 and the other where the velocity is related to the binding energy so that v = 0 when r = ∞. The latter co-ordinate system has a better physical basis as it is directly connected to the confinement time and hence it will be adopted giving:

$$v_r^2 = \frac{2e \, \Delta\phi}{m_e} = \frac{2e}{m_e} (\phi_w + \phi(r))$$

where v_r now represents the velocity required to overcome the binding energy

when the electron is at its turning points (where it is most of the time).

A first approximation to the potential distribution with respect to radius may be made by assuming it also to be gaussian but with a different radius r_o/β, so that

$$\phi(r) = - \phi_w . \left[1 - \exp\left(- (\beta r/r_o)^2\right) \right] \qquad \ldots (8)$$

This approximation is strongly supported by experiment and also by the full numerical solution of Poissons equation which replaces equation 8. Hence:

$$v_r^2 = \frac{2e\phi_w}{m_e} \exp\left(-\left(\frac{\beta r}{r_o}\right)^2\right) = v_m^2 \exp\left(-\left(\frac{\beta r}{r_o}\right)^2\right)$$

The other co-ordinate system for v gives an identical electron distribution, but breaks down at large values of r because of the approximation assumed for ϕ.

Returning to equation 7, it can be seen that A must be zero and if the dependence of D_v on n_e is included, then on integration the equation becomes:

$$Cn_v^2 = \frac{nn_{bo}\,\sigma_i v_b r_o^4}{\beta^2(2/\beta^2 - 2)} \left(\frac{v^2}{v_m^2}\right)^{1/\beta^2} \cdot \frac{1}{v^2} + B$$

When the transform is applied in reverse, the electron density in real space may be obtained:

$$Cn_e^2 = \frac{nn_{bo}\sigma_i v_b \beta^2 v_m^2}{(2/\beta^2 - 2)} \exp(- r^2/r_o^2) . \exp - (\beta r/r_o)^2 + \frac{B\beta^4}{r_o^4} v_m^2 \exp - (\beta r/r_o)^2$$

However, the electron density is expected to decrease more rapidly than the potential, hence the numerical constant of integration, B, must be zero. The final solution for the electron density is:

$$n_e = \left[\frac{4\beta^2\pi}{0.97(2/\beta^2 - 2)} \cdot \frac{\varepsilon_o^2}{e^3 \ell n \Lambda} \cdot \left(\frac{2eT}{m_e}\right)^{\frac{1}{2}} nn_{bo}\sigma_i v_b m_e \phi_w\right]^{\frac{1}{2}} \exp - \frac{(1+\beta^2)r^2}{2r_o^2} \qquad \ldots (9)$$

This solution is based on the assumption that the potential well has a gaussian shape of radius r_o/β. Equation 9 above shows that the radius of the electron distribution is, as would be expected, intermediate between the beam radius r_o and the potential radius and is $r_o(2/(1+\beta^2))^{\frac{1}{2}}$.

It has been assumed that the trapped electrons have a Maxwellian distribution whereas in reality this distribution will be truncated at the velocity v_m which causes the tail of the distribution to be lost. Virtually no electrons whose velocity exceeds v_m will be present as the electron transit time is shorter than one percent of the collision time. The truncated distribution function can be found using a method developed by Cordey [9] which gives:

$$n_e = n_{eo} \int_{\varepsilon=\phi}^{\varepsilon=\phi_w} c^2 \exp - \varepsilon/T \, dc \Big/ \int_{\varepsilon'=0}^{\varepsilon'=\phi_w} c^2 \exp - \varepsilon'/T \, dc$$

where $\varepsilon = m_e c^2/2e - \phi$ and $\varepsilon' = m_e c^2/2e$. This may be solved to give:

$$n_e = n_{eo} \left[\frac{(\pi/4)^{\frac{1}{2}} \operatorname{erf} (\sqrt{(\phi_w + \phi)/T}) \exp(\phi + \phi_w)/T - \sqrt{(\phi + \phi_w)/T}}{(\pi/4)^{\frac{1}{2}} \operatorname{erf} (\sqrt{\phi_w/T}) \exp \phi_w/T - \sqrt{\phi_w/T}} \right]$$

which is the truncated Maxwellian distribution of electrons in a well of finite depth.

Curves of n_e/n_{eo} are shown in Fig. 1 for several values of ϕ_w/T. A more tractable form of the above equation is obtained by numerical approximation to the above curves yielding

$$n_e = n_{eo} \exp(\phi/T) . (\phi + \phi_w)/\phi_w \qquad \ldots (10)$$

This is also used in the numerical analysis discussed in section 5.

It is clear that the distribution functions in equations 9 and 10 must be made identical. This is achieved through the correct choice of β which in turn involves the consideration of the energy balance of the system in order to determine T. However knowledge of β is not required in the derivation of n_{eo}, the electron density on axis which can be obtained by inspection. If

equations 9 and 10 are combined then;

$$n_e = \left[\frac{4\beta^2}{0.97(2/\beta^2-2)} \frac{\pi\varepsilon_o^2}{e^3 \ell n\Lambda} \left(\frac{2eT}{m_e}\right)^{\frac{1}{2}} nn_{bo}\sigma_i y_b m_e \phi_w\right]^{\frac{1}{2}} \exp\frac{\phi}{T} \cdot \left(\frac{\phi_w+\phi}{\phi_w}\right) \quad \ldots (11)$$

The above expression shows that the value of β has only a small influence on the electron distribution.

4. THE ELECTRON DISTRIBUTION AND ENERGY BALANCE

The energy balance of the beam plasma may be reduced to equating the energy loss arising from the escaping slow ions to the energy absorbed by the electrons arising from coulomb collisions with the beam. The energy removed by slow ions produced by charge exchange does not enter into this energy balance because this energy comes from the electrostatic deceleration of the beam by its own potential well. In addition the electrons cannot remove their kinetic energy, eT, from the beam as they escape when their energy just exceeds the binding potential.

The irreversible energy loss of the beam ions, when they pass through an electron gas, is critically dependent on the velocity distribution of the electrons and is maximum when the electron velocity is close to zero. In the previous section the electron velocity distribution was assumed to be Maxwellian with a cut-off at $v^2 = 2e\phi_w/m_e$. This cut-off occurs at a velocity greater than v_b and hence will not affect the energy absorption. However it is possible to show (see section 4.3) that the energy absorbed by a true Maxwellian distribution of temperature, T, during the containment time, is approximately an order of magnitude smaller than that required to escape. This arises from the high thermal velocity of the electrons which has been measured to be approximately twice the beam velocity.

Consequently another process is responsible for the energy absorption and it will be demonstrated below that the electron distribution function at low velocities is considerably modified by the presence of newly created electrons which have low velocities and can hence act as good energy absorbers for the whole distribution. However the number density of this group of electrons is

low as they quickly thermalize with the main distribution.

The density and distribution function of these electrons can be evaluated from the Fokker-Planck equation. This function can then be used in the beam deceleration equation which determines the energy loss from the beam and hence equated to the energy removed by the slow ions.

A simple method showing the physics underlying this approach is shown in fig. 2. The beam energy and newly created electrons enter the perturbed distribution. These electrons gain energy from the main distribution and also transfer energy and particles via the heated electrons which are absorbed into the main distribution. In this way the total energy and particle content of the perturbed distribution remains constant in time to give a steady state solution. Finally the main Maxwellian distribution loses electrons which evaporate from the beam and also remove their binding energy from the beam thus maintaining the energy and particle content of this distribution.

4.1 The Fokker-Planck Equation

It is assumed in the following analysis that the electron distribution is isotropic, in which case the general Fokker-Planck equation takes the form:

$$\left(\frac{\partial f}{\partial t}\right)_c = \frac{\Gamma}{v^2}\left\{-\frac{\partial}{\partial v}\left(fv^2\frac{\partial h}{\partial v} + f\frac{\partial g}{\partial v}\right) + \frac{1}{2}\cdot\frac{\partial^2}{\partial v^2}\left(fv^2\frac{\partial^2 g}{\partial v^2}\right)\right\} \qquad \ldots (12)$$

which has been derived by Rosenbluth et al.[10]. In this equation, f represents the total electron distribution function and v is the electron speed. Hence the electron density, n_e, is:

$$n_e = \int_o^\infty f.4\pi v^2 dv$$

Also the terms Γ, h and g are determined by the equations:

$$\Gamma = e^4 \ell n\Lambda/4\pi\,\varepsilon_o^2 m_e^2$$

$$h(v) = \sum_j \frac{m_e + m_j}{m_j}\left\{\frac{4\pi}{v}\int_o^v f_j v'^2 dv' + 4\pi\int_v^\infty f_j v' dv'\right\} \qquad \ldots (13)$$

$$g(v) = \sum_j \frac{4\pi}{3v} \int_o^v f_j v'^2 (3v^2 + v'^2) dv' + \frac{4\pi}{3} \int_v^\infty f_j v' (3v'^2 + v^2) dv' \quad \ldots (14)$$

It is impossible to solve equation 12 analytically for a general distribution function, but, if it is assumed that the electron distribution function is essentially a perturbed Maxwellian (because the containment time is a few times the collision time for electrons), then the equation may be linearized. The effects of the source of electrons created by ionization can be viewed as a perturbation and the total distribution function can be represented by

$$f = \left(\frac{m_e}{2e\pi T}\right)^{3/2} \cdot n_e \cdot \exp\left(-\frac{m_e v^2}{2eT}\right) + f_n$$

where f_n is the perturbation. The Maxwellian function is a stationary state of the Fokker-Planck equation and hence it makes no contribution to the time derivative on the L.H.S. The perturbation distribution, f_n, is assumed to be too small to interact with itself via the h and g parameters.

The time dependent part of the Fokker-Planck equation hence represents the rate of loss of electrons from any element of velocity and real space, which becomes, for electron creation in the ion beam,

$$\left(\frac{\partial f}{\partial t}\right)_c = - S(v) \cdot \frac{dN_e}{dt} \quad \ldots (15)$$

where dN_e/dt is the rate of appearance of new electrons per unit volume taking into account their orbitals around the beam axis. The function S(v) represents the velocity distribution of the new electrons at a point in real space arising from their potential energy. It is shown in appendix II that dN_e/dt depends critically on the initial velocity of creation of the electrons which has been measured experimentally by Rudd and Jorgensen [11].

In this instance (see appendix II)

$$\frac{dN_e}{dt} = n n_b \sigma_i v_b \frac{4r}{\sqrt{\pi} r_o} \frac{e\phi_o}{m_e v_b^2}$$

where ϕ_o is the potential at r_o.

The electron velocity distribution, S(v) can be derived from the beam profile and potential distribution. As the main area of interest is near the axis, the gaussian potential well can be approximated to a parabolic well so that

$$\frac{m_e v^2}{2} = e\Delta\phi + \frac{m_e w^2}{2}$$

$$= \frac{e\phi_o}{r_o^2}(p^2 - r^2) + \frac{m_e w^2}{2}$$

where r is the radius where S(v) is determined and w is the initial electron velocity. The probability of a velocity v depends on the distribution of both w and p as shown in the equation below:

$$S(v) = \frac{\int_o^v f(w) \cdot g(p)\, dw}{4\pi v^2 \int_o^\infty \int_o^v f(w)\, g(p)\, dw\, dv}$$

It is assumed that f(w) is $2w \exp(-w^2/w_o^2)/w_o^2$ where w_o is the characteristic initial velocity (experimentally $w_o \simeq v_b$) and g(p) is exp $- p^2/r_o^2$ which is derived from the beam profile. As $w_o^2 < 2e\phi_o/m$, integration gives:

$$S(v) \simeq \frac{1}{2\pi^{3/2}} \left(\frac{m_e}{2e\phi_o}\right)^{\frac{1}{2}} \cdot \frac{1}{v^2} \cdot \exp\left(-\frac{m_e v^2}{2e\phi_o}\right)$$

which has some similarity to a Maxwellian distribution.

When equation 15 is combined with equation 12, the Fokker-Planck equation becomes:

$$- nn_b \sigma v_b \cdot \frac{2}{\pi^2} \frac{r}{r_o} \left(\frac{e\phi_o}{m_e v_b^2}\right)\left(\frac{m_e}{2e\phi_o}\right)^{\frac{1}{2}} \frac{\exp(-m_e v^2/2e\phi_o)}{v^2}$$

$$= \frac{\Gamma}{v^2}\left[-\frac{\partial}{\partial v}\left(f_n v^2 \frac{\partial h}{\partial v} + f_n \frac{\partial g}{\partial v}\right) + \frac{1}{2}\frac{\partial^2}{\partial v^2}\left(f_n v^2 \frac{\partial^2 g}{\partial v^2}\right)\right]$$

It is possible to integrate this equation once by multiplying by $4\pi v^2 dv$ and integrating over the range 0 to v which yields:

$$- nn_b \sigma v_b \frac{4}{\pi^{\frac{1}{2}}} \frac{e\phi_o r}{m_e v_b^2 r_o} \operatorname{erf}\left(\frac{m_e v^2}{2e\phi_o}\right)^{\frac{1}{2}} = 4\pi\Gamma\left[- f_n\left(v^2 \frac{\partial h}{\partial v} + \frac{\partial g}{\partial v}\right) + \frac{1}{2} \frac{\partial}{\partial v}\left(f_n v^2 \frac{\partial^2 g}{\partial v^2}\right)\right] \quad \ldots (16)$$

The next integration depends on the functions h and g which can be derived from equations 13 and 14 and the distribution functions of each species of particle.

4.1.1. The h function

There are three species of particles, namely the main electron distribution, which is maxwellian, the slow ions and the beam ions. The distribution functions of the electrons and beam ions are respectively:

$$f_e = n_e\left(\frac{m_e}{2\pi eT}\right)^{3/2} \exp - \frac{m_e v^2}{2eT} \quad \ldots (17)$$

$$f_b = \delta(v - v_b)\ \delta(\mu - 1)/4\pi v^2 \quad \ldots (18)$$

where δ is the delta function and μ equals cos θ in polar co-ordinates. This anistropy of the beam must be removed by integration over θ before it can be substituted into equation 12, but it is useful to perform this operation after h_b and g_b have been derived in order to improve the accuracy of the expression.

The slow ion function is more difficult to derive, but it will be shown shortly that the dispersion caused by these particles is unimportant because of the small value of n_i. A simple form for f_i is to assume it to be Maxwellian with a characteristic energy of $e\phi_o$ so that the ion velocity is far smaller than the initial electron velocity. Hence

$$f_i = n_i\left(\frac{m_i}{2\pi e\phi_o}\right)^{3/2} \exp\left(- \frac{m_i v^2}{2e\phi_o}\right) \quad \ldots (19)$$

Substitution of these expressions in equation 13 gives:

$$h_e = \frac{2n_e}{v} \cdot \operatorname{erf}(m_e v^2/2eT)^{\frac{1}{2}} \approx 2n_e\left\{\frac{2}{\sqrt{\pi}}\left(\frac{m_e}{2eT}\right)^{\frac{1}{2}} - \frac{2v^2}{3\sqrt{\pi}}\left(\frac{m_e}{2eT}\right)^{3/2} + \ldots\right\}$$

$$h_i = m_e n_i / v m_i$$

as $v >> (2e\phi_o/m_i)^{\frac{1}{2}}$ and $m_i >> m_e$.

$$h_b = \frac{m_e n_b}{2m_b} (v^2 + v_b^2 - 2vv_b\mu)^{-\frac{1}{2}}$$

This last expression is derived from the expanded version of equation 13 given by Rosenbluth et al [10]. However the dependence on μ is inconvenient in the assumed isotropic distribution, f_n, and maybe eliminated by interaction over all values of μ from 1 to - 1. In this case

$$\bar{h}_b = \frac{m_e n_b}{8m_b v_b v} \left\{ |v + v_b| - |v - v_b| \right\}$$

These three expressions for h represent the relative magnitude of the deceleration of the newly created electrons by friction or scattering with the beam ions, slow ions and the main electron distribution. In view of the mass ratio which enters into this type of effect, it is to be expected that beam ions are virtually ineffective in slowing down the electrons (the beam ions are incapable of producing any deceleration until the electron velocity exceeds that of the beam). In this case the value of $v^2 \partial h/\partial v$ is:

$$v^2 \partial h/\partial v = v^2 \partial h_e/\partial v = \frac{-8n_e}{3\pi^{\frac{1}{2}}} v^3 \left(\frac{m_e}{2eT}\right)^{3/2} + \ldots \qquad \ldots (20)$$

4.1.2. The g function

Using the expressions developed above for f_e, f_i and f_b it can be shown with the aid of equation 14 that:

$$g_e = \frac{n_e}{4v} \left(\frac{2eT}{m_e}\right) \left[\frac{4v}{\pi^{\frac{1}{2}}} \left(\frac{m_e}{2eT}\right)^{\frac{1}{2}} \exp - \frac{m_e v^2}{2eT} + 2\left(1 + \frac{m_e v^2}{eT}\right) \operatorname{erf}\left(\frac{m_e v^2}{2eT}\right)^{\frac{1}{2}} \right]$$

$$\approx \frac{n_e}{4} \left(\frac{2eT}{m_e}\right)^{\frac{1}{2}} \left\{ \frac{8}{\pi^{\frac{1}{2}}} + \frac{8}{3\pi^{\frac{1}{2}}} \frac{m_e v^2}{2eT} + \frac{1.47}{\pi^{\frac{1}{2}}} \left(\frac{m_e v^2}{2eT}\right)^2 + \ldots \right\}$$

$$g_i \simeq n_i v \text{ if } v >> (2e\phi_o/m_i)^{\frac{1}{2}}$$

$$g_b = \frac{n_b}{2} (v^2 + v_b^2 - 2vv_b\mu)^{\frac{1}{2}}$$

Hence;

$$\bar{g}_b = \frac{n_b}{12vv_b} \left\{ |v + v_b|3 - |v - v_b|^3 \right\}$$

This last expression is obtained by averaging over all values of μ.

Again the scattering effects of the slow ions may be neglected but the scattering caused by the electron distribution and the beam ions are comparable and both must be included. The scattering represented by the g expression will cause the average energy of the newly created electrons to rise. In the first order the derivative of g with velocity is:

$$\partial g/\partial v = \frac{\partial g_e}{\partial v} + \frac{\partial g_b}{\partial v} = \frac{4n_e}{3\pi^{\frac{1}{2}}} \left(\frac{m_e v}{2eT}\right) \cdot \left(\frac{2eT}{m_e}\right)^{\frac{1}{2}} + \frac{n_b v}{3v_b} \qquad \ldots (21)$$

4.2 The Perturbed Distribution Function

With the values of g and h in equations 20 and 21, it is possible to solve equation 16 which gives on integration

$$f_n v^2 \frac{\partial^2 g}{\partial v^2} \exp\left(- 2 \int_v \frac{v'^2 \partial h/\partial v' + \partial g/\partial v' \, dv'}{v'^2 \partial^2 g/\partial v'^2}\right) + \frac{2nn_b \sigma v_b r}{4\pi \Gamma r_o}$$

$$x \frac{4}{\pi^{\frac{1}{2}}} \frac{e\phi_o}{m_e v_b^2} \int_v \operatorname{erf}\left(\frac{m_e u^2}{2e\phi_o}\right)^{\frac{1}{2}} \cdot \exp\left(- 2 \int_u \frac{v'^2 \partial h/\partial v' + \partial g/\partial v'}{v'^2 \partial^2 g/\partial v'^2} dv'\right) du = \text{constant.}$$

Substitution of equations 20 and 21 show that $v^2 \partial h/\partial v$ is unimportant compared with $\partial g/\partial v$ which suggests that the deceleration of the newly created electrons is unimportant compared with the scattering collisions. In this case the above equation may be simplified to:

$$f_n \frac{\partial^2 g}{\partial v^2} + \frac{2nn_b \sigma v_b r}{4\pi \Gamma r_o} \cdot \frac{4}{\sqrt{\pi}} \frac{e\phi_o}{m_e v_b^2} \int_v \operatorname{erf}\left(\frac{m_e u^2}{2e\phi_o}\right)^{\frac{1}{2}} \cdot \frac{du}{u^2} = \text{constant}$$

If u is small, then:

$$f_n = C - \frac{nn_b \sigma_i v_b r}{4\pi \Gamma r_o} \cdot \frac{8}{\pi} \left(\frac{2e\phi_o}{m_e}\right)^{\frac{1}{2}} \frac{\ell n v}{v_b^2} \left[\frac{4n_e}{3\pi^{\frac{1}{2}}} \left(\frac{m_e}{2eT}\right)^{\frac{1}{2}} + \frac{n_b}{3v_b}\right]^{-1}$$

The constant C is of some importance as no sink of electrons has been postulated. A natural sink exists when v is of the order of the thermal velocity of the electrons as then the two distributions cannot be distinguished. If f_n is zero when v equals v_s then:

$$f_n = A\ell n(v_s/v)$$

$$\text{where } A = \frac{nn_b\sigma_i r}{4\pi\Gamma r_o} \cdot \frac{8}{\pi} \left(\frac{2e\phi_o}{m_e v_b^2}\right)^{\frac{1}{2}} \cdot \left[\frac{4n_e}{3\pi^{\frac{1}{2}}} \left(\frac{m_e}{2eT}\right)^{\frac{1}{2}} + \frac{n_b}{3v_b}\right]^{-1} \qquad \ldots (22)$$

The total number density of these electrons can be found by integration over velocity space which gives:

$$n_n = \int_o^{v_s} f_n . 4\pi v^2 dv = \frac{4\pi\, A v_s^3}{9}$$

When v_s is less than $(2eT/m_e)^{\frac{1}{2}}$ this density is considerably smaller than n_e. It is difficult to determine the value of v_s precisely, but if v equals v_s when the scattering time for these new electrons with themselves is equal to the scattering time for collisions between new electrons and the main distribution, then v_s is approximately $\frac{1}{2}(2eT/m_e)^{\frac{1}{2}}$ although this velocity depends on the gas and beam densities. An illustration of the distribution function is shown in Fig. 3 where the perturbation appears as a spike on the Maxwellian distribution function at v = 0. The effect of the uncertainty in the value of v_s does not influence the energy transfer however as will be seen in the next section.

4.3 The Beam Energy Balance

The deceleration of the beam is governed by an equation of the type:

$$\frac{\partial v_b}{\partial t} = \Gamma_b \frac{\partial H}{\partial v_b}$$

where $\Gamma_b = e^4 \ell n\Lambda / 4\pi\varepsilon_o^2 m_b^2$

and

$$H(v_b) = \sum_j \frac{m_b + m_j}{m_b} \left[\frac{4\pi}{v_b}\int_o^{v_b} v'^2 f_j dv' + 4\pi\int_{v_b}^{\infty} v' f_j dv'\right]$$

The slow ions are ineffective in retarding the beam ions because of their high mass but both electron distributions can cause deceleration. Substitution of f_m and f_n in the above equation yields:

$$H = \frac{m_b}{m_e}\left[\frac{n_e}{v_b}\ \text{erf}\ (m_e v_b^{\,2}/2eT)^{\frac{1}{2}} + 4\pi A\left(-\frac{5v_b^{\,2}}{36} - \frac{v_b^{\,2}}{6}\,\ell n\ v_s/v_b + \frac{v_s^{\,2}}{4}\right)\right]$$

If the electron temperature is high then the contribution from the main distribution is small (because $\omega > v_b$) and hence can be neglected. Substitution of experimental values shows that less than 10% of the total energy input to the electrons comes from this channel. Hence, in this case, the rate of change of beam energy is:

$$\frac{dU_b}{dt} = 2m_b v_b \frac{dv_b}{dt} = -\ 4\pi A\ m_b \frac{v_b^{\,2}}{3}\ \frac{m_b \Gamma_b}{m_e}\left(2\ell n(v_s/v_b) + 4/6\right)$$

and

$$\frac{dW_e}{dt} = -\ n_b \frac{dU_b}{dt} = \frac{4\pi}{3} A n_b \frac{m_b^{\,2} v_b^{\,2}}{m_e} \Gamma_b \cdot \left(2\ell n(v_s/v_b) + 4/6\right) \qquad \ldots\ (23)$$

The value of v_s has little effect on the energy transfer.

The last stage involves the integration of the energy absorbed in a unit volume at r, represented by dW_e/dt, over all radii which is equal to the total energy removed by the flux of escaping ions. This balance may be represented by the expression:

$$\int_o^\infty n n_b \sigma_i v_b\ e\phi_w\ \exp -\frac{\beta^2 r^2}{r_o^{\,2}} \cdot 2\pi r dr = \int_o^\infty \frac{dW_e}{dt} \cdot 2\pi r dr$$

This integration is necessary because the electron-electron energy transfer time is considerably shorter than the containment time. It is not possible to solve exactly the right hand side of the above equation, but the term A can be expanded as a series function of the ratio n_b/n_e. Hence after simplification:

$$\frac{\phi_w}{1+\beta^2} = \frac{2\,\phi_o^{\frac{1}{2}}\,T^{\frac{1}{2}}\,n_{bo}}{(2-(1+\beta^2)/2)\,n_{eo}} \cdot (2\ell n(v_s/v_b) + 2/3)$$

$$\times \left[1 - \frac{(3/2 - \beta^2/2)}{(2-\beta^2)} \frac{\pi^2}{4} \frac{n_{bo}}{n_{eo}} \left(\frac{2eT}{m_e v_b^2}\right) + \ldots\right]$$

The higher order terms in n_{bo}/n_{eo} may be collected to give:

$$\frac{\phi_w}{1+\beta^2} \simeq \frac{2\,\phi_o^{\frac{1}{2}}\,T^{\frac{1}{2}}}{(2-(1+\beta^2)/2)} \frac{n_{bo}}{n_{eo}} (2\ell n(v_s/v_b) + 2/3) \cdot \left[1 - \frac{\pi^{\frac{1}{2}}}{10} \frac{n_{bo}}{n_{eo}} \frac{2eT}{m_e v_b^2}\right]$$

if $\beta \simeq 0.33$ (see next section). The small value of n_b/n_e at large values of r attenuates the second term considerably and at high pressures (greater than 10^{-4} torr), it can be neglected completely.

4.4 The β Parameter

β^2 has been a free parameter in the model, although an exact theory could determine β^2 vis a numerical solution of an integro-differential equation based on velocity space diffusion and energy balance. The approach adopted here is considerably simpler and offers a greater insight into the meaning of the β parameter.

In section 3.2, β^2 was to be determined by the equality between the radial dependence of n_e in equations 10 and 11. This demands that

$$\exp - \frac{(1+\beta^2)}{2} \frac{r^2}{r_o^2} = \frac{\phi + \phi_w}{\phi_w} \exp \frac{\phi}{T}$$

where ϕ is the potential relative to the centre of the beam. Hence, near the axis where ϕ is small

$$-\frac{(1+\beta^2)r^2}{2r_o^2} = \frac{\phi}{T}$$

$$\approx -\frac{\phi_w}{T}\left(1 - \exp - \left(\frac{\beta r}{r_o}\right)^2\right) \qquad \ldots (24)$$

If n_{eo} is approximately equal to n_{bo} and only the first term of the series

expansion of the exponential in equation 24 is considered then the above equality becomes:

$$\frac{1 + \beta^2}{2} = \left(\frac{2\beta(1 + \beta^2)(1 - e^{-\beta^2})^{\frac{1}{2}}}{(3 - \beta^2)/2} \times \left(2\ell n(v_s/v_b) + 2/3\right) \right)^2$$

The solution to this is $\beta^2 = 0.33$ when v_s/v_b equals 1.4 although β is relatively invariant to the value of v_s/v_b.

With this calculated value of β^2, it is possible to write:

$$\phi_w = 2.02 \left(\frac{n_{bo}}{n_{eo}}\right)^2 T \left(1 - 0.4 \frac{n_{bo}}{n_{eo}} \frac{w}{v_b}\right)^2 \qquad \ldots (25)$$

If this equation is combined with equation 11, it is possible to eliminate T giving:

$$n_{eo} = 0.33 \pi \varepsilon_o{}^2 (e m_e)^{\frac{1}{2}} n \sigma_i v_b \phi_w{}^{3/2}/e^3 \ell n(\Lambda) \qquad \ldots (26)$$

4.5 Radial and Axial Energy Transfer

It has been assumed, hitherto, that the beam is perfectly collimated and the electron temperature is uniform everywhere. It will be shown here that a gaussian beam profile allows the expressions developed for perfectly collimated beams to be extended to divergent beams. In addition the value of β^2 derived in the previous section allows the local rate of energy absorption, dW_e/dt, to have exactly the same radial scaling as the energy loss caused by the outward drift of the electrons.

4.5.1 Axial Energy Transfer

The effects of beam divergence cause an axial variation of ϕ_w, producing a broad shallow well where the beam is wide which is transformed into a deep narrow well near the beam extraction region. The electrons can move axially along the well oscillating between contours of constant potential. The electron production rate, Q_e, in a zone $d\phi$ at potential ϕ for a local beam density, n_b, is:

$$Q_e = n n_b \sigma v_b \cdot 2\pi r \frac{dr}{d\phi} d\phi$$

For a beam and potential well which are both gaussian

$$\phi = \phi_w \exp - (\beta r/r_o)^2$$

$$n_b = n_{bo} \exp - r^2/r_o^2$$

$$= n_{bo} (\phi/\phi_w)^{1/\beta^2}$$

and

$$dr/d\phi = r_o^2/2r\beta^2\phi$$

where ϕ is in this case the binding potential of the electrons and is measured from the remote walls which are at constant potential. Hence:

$$Q_e = n\sigma_i n_{bo} v_b \cdot \frac{\pi r_o^2}{\beta^2 \phi} \left(\frac{\phi}{\phi_w}\right)^{1/\beta^2} d\phi$$

However the beam current remains constant along the beam axis so that

$$I_b = \pi n_{bo} v_b e\, r_o^2$$

and

$$Q_e = \frac{n\sigma I_b}{\beta^2 e\phi} \left(\frac{\phi}{\phi_w}\right)^{1/\beta^2} d\phi$$

Hence if the beam current and gas density are constant along the beam axis then the production rate of electrons along a contour of constant potential is the same irrespective of beam size. Hence there is no axial flow of electrons and the energy balance of an axial segment of the beam can be considered as if it were infinitely long and of the same radius. This arises from the gaussian profile of the beam which in turn generates a similar potential distribution. In this state the flow of particles (and hence energy) along the axis is zero.

4.5.2 Radial Transfer

The energy absorbed per unit volume by the electron distribution is determined by the function dW_e/dt. This energy is absorbed by the local electrons and enables them to drift outwards against the electric field. If the radial dependence of dW_e/dt and the energy required to maintain this drift

are the same then this implies that there is no temperature gradient because the local energy absorption and loss are the same everywhere. From equation 23 the radial scaling of dW_e/dt is:

$$\frac{dW_e}{dt} = C \cdot \frac{r}{r_o} \exp - \frac{2r^2}{r_o^2} \cdot \exp \frac{(1 + \beta^2)}{2} \frac{r^2}{r_o^2}$$

where C contains all terms which are not functions of r. The energy required for drift against the field is: $n_e E.(dr/dt)_d$ where E is the local electric field and $(dr/dt)_d$ is the drift velocity. An approximate expression for this velocity is:

$$(dr/dt)_d \simeq n_b n \sigma_i v_b r_o / n_e$$

Hence the radial dependence of this energy loss is:

$$\text{loss rate} = n n_{bo} \sigma_i v_b r_o \frac{2\phi_w r}{r_o^2} \exp - \frac{\beta^2 r^2}{r_o^2} \cdot \exp - \frac{r^2}{r_o^2}$$

These two radial expressions are exactly the same provided:

$$1.5 - \beta^2/2 = 1 + \beta^2$$

or

$$\beta^2 = 0.33$$

This value of β^2 is in exact agreement with the value derived in section 4.4. from a completely different concept.

Hence it can be seen that there will be a strong tendency for a beam of any arbitary profile to relax into a gaussian shape where β^2 is 0.33. This profile eliminates any need for axial or radial energy transport and hence is an equilibrium state for the beam plasma.

5. POISSONS EQUATION

The electrostatic potential can be derived from the charge densities and electron temperature by two methods. The exact method is to solve the full Poisson's equation in cylindrical geometry, which will be done in a following section. A less accurate technique involves the assumption of plasma neutrality

so that $d^2\phi/dr^2$ and $d\phi/dr$ are neglected and Poisson's equation reduces to

$$n_b + n_i = n_e$$

which is the plasma equation. Harrison and Thompson [12] have solved the plasma equation when n_b is zero and Green [7] has produced solutions where n_b is finite and uniform. This equation will give a detailed spatial solution when the Boltzmann distribution for electrons is assumed (i.e. $n_e = n_{eo} \exp + \phi/T$). The validity of the plasma equation is doubtful, however, at low pressure because of the dominant effects of the beam ions and the high potential gradients in the plasma.

A much simpler solution of the plasma equation is described by Gabovich et al where only axial plasma neutrality is assumed and all radial variation in density is neglected. This determines the magnitude of the potential well but not its shape. A similar technique will be used in the next section to obtain an approximate estimate for the scaling of ϕ_w.

5.1 Neutral Plasma Solution

The basic expression equates n_{eo} to $n_{io} + n_{bo}$, hence from equations 3 and 26 one obtains:

$$0.33 \frac{\phi_w^{3/2} \pi\varepsilon_o^2 (em_e)^{\frac{1}{2}} n\sigma_i v_b}{e^3 \ell n\Lambda} = \left(\frac{m_i}{2e\phi_w}\right)^{\frac{1}{2}} \frac{n_{bo} n v_b \sigma r_o}{(1 - \exp -\beta^2)} + n_{bo} \quad \ldots (27)$$

The above equation relates the potential to the gas density and beam density and indicates that, at low pressures:

$$\phi_w = (n_{bo}/n)^{2/3} \left[\sigma_i v_b \cdot 0.33 \pi\varepsilon_o^2 \frac{(m_e e)^{\frac{1}{2}}}{e^3 \ell n\Lambda}\right]^{-2/3} \quad \ldots (28a)$$

and at high pressures:

$$\phi_w^2 = n_{bo} r_o \frac{\sigma}{\sigma_i} \left(\frac{m_i}{m_e}\right)^{\frac{1}{2}} \frac{e^2 \ell n\Lambda}{0.33 \pi\varepsilon_o^2} \frac{1}{(1 - e^{-\beta^2})} \quad \ldots (28b)$$

These two equations show that ϕ_w decreases with increasing pressure until a lower limit is reached, which is determined by the production rate of the slow ions. Furthermore at low pressures, the beam potential depends solely on the beam density and is independent of the beam radius. This scaling differs completely from the scaling of the potential of a vacuum beam where

$$\phi_{wv} \propto n_b r_o^2$$

This effect may be exploited to produce an extremely collimated beam whose divergence is only limited by its finite emittance. These results are mentioned in Section 6.3 and are discussed in greater detail elsewhere (Holmes and Thompson [13].

At high gas target thicknesses, a large fraction of the ion beam (dependent on the beam energy) will be converted into neutral atoms and this neutral atom beam cannot create a potential well. This fast neutral beam is a source of plasma and therefore a sheath appears at the plasma boundary (i.e. the walls). Dunn and Self [6] have discussed this problem in detail for finite temperature electrons in electron beams. This treatment has been extended by Green [7] to intense ion beams. Hence by a simple modification of the model to incorporate the relative magnitudes of n_{bo} to n_{no}, the fast neutral density, it can be shown that:

$$\phi_{wi} = \phi_w \cdot \left(\frac{n_{no} + n_{bo}}{n_{bo}}\right)^{2/3} \quad \text{at low pressure}$$

$$\phi_{wi} = \phi_w \cdot \left(\frac{n_{no} + n_{bo}}{n_{bo}}\right) \quad \text{at high pressure}$$

where ϕ_{wi} is the potential generated by a pure ion beam of density $(n_{bo} + n_{no})$.

5.2 The Numerical Solution

Poissons equation in cylindrical geometry is of the form:

$$\frac{d^2\phi}{dr^2} + \frac{1}{r}\frac{d\phi}{dr} = -\frac{e}{\varepsilon_o}(n_i + n_b - n_e) \qquad \ldots (29)$$

where there is azimuthal and axial uniformity in potential. Each charge species has a different spatial distribution which is described by equations 2, 7 and 11 and these can be introduced into equation 29. This discussion is limited to a gaussian beam profile which is the steady state solution following the arguments advanced in sections 4.4 and 4.5. However it is easy to apply this technique (assuming that the other particle profiles are independent) to other primary beam profiles. For a gaussian beam, however, equation 29 becomes:

$$\frac{\varepsilon_o}{e}\left(\frac{d^2\phi}{dr^2}+\frac{1}{r}\frac{d\phi}{dr}\right)=-\left[\frac{n\sigma\, v_b}{r}\left(\frac{m_i}{2e}\right)^{\frac{1}{2}}\int_o^r \frac{n_{bo}\exp - a^2/r_o^2\ ada}{\left(\phi(a)-\phi(r)\right)^{\frac{1}{2}}}\right.$$

$$\left. + n_{bo}\exp\left(-r^2/r_o^2\right) - n_{eo}\exp\left(\phi/T\right).\left(\phi_w+\phi/\phi_w\right)\right]$$

This equation may be slightly simplified by the introduction of the variables $x = r/r_o$ and $y = \phi/\phi_o$. Hence:

$$-\frac{\varepsilon_o\phi_o}{er_o^2}\left(\frac{d^2y}{dx^2}+\frac{1}{x}\frac{dy}{dx}\right)=\frac{n_{io}}{x}\int_o^x\frac{e^{-x'^2}\,x'\,dx'}{(y'-y)^{\frac{1}{2}}}-n_{eo}\exp\frac{\phi_o y}{T}\cdot\left(\frac{\phi_w+y\phi_o}{\phi_w}\right)+n_{bo}\,e^{-x^2} \quad \ldots (30)$$

It is possible to solve this integro-differential equation using a finite step technique to approximate the differentials. However a single solution to Poisson's equation is insufficient to determine the well potential because n_{eo}, T and n_{io} are all functions of ϕ_w. Hence a relaxation routine must also be included in the numerical solution so that the value of ϕ_w derived from Poissons equation is used to modify the initial estimates for n_{eo}, T and n_{io}. The final numerical solution is shown in figs. 4 and 5 where particle and potentials distributions in both pressure regimes are shown.

It can be seen that the three charged particle distributions and the potential well are all of gaussian form although with different radii. The shape of the numerical potential well supports the arguments advanced in Section 3.2.

6. EXPERIMENTAL RESULTS

A series of experiments have been performed on a helium beam moving at constant energy through a helium gas cell. An illustration of the apparatus is shown in fig. 6. The beam is produced by a four electrode extraction system which has been described by Thompson[14] and the current density and divergence angle of the beam may be controlled by varying the plasma density in the source. No magnetic focussing of the beam is used. The beam plasma is isolated from the extraction electrodes by the last electrode gap which creates a potential to reflect the electrodes back into the plasma. Thus the beam plasma is surrounded on all sides by surfaces at a uniform potential (in this case these surfaces are earthed) and electrons can only escape by velocity space diffusion.

Two techniques are used to examine the space charge potential. Firstly the plasma potential may be measured using a "hot" Langmuir probe, described by Gabovich [4]. The bias voltage relative to the earthed wall required to give zero wall current from the probe is equal to the local plasma potential. Secondly a shielded probe with a grid may be used to make an energy analysis of the particles which are expelled radially from the beam. This probe does not give a spatial resolution of the potential well and can only determine the electron temperature and maximum well potential from the energy distribution of the slow current. It has the advantage that it does not enter the beam and hence can work at high beam energies.

6.1 The Potential Well

The plasma potential at a point in the beam is defined as the voltage between the measurement point and the beam axis and is equal to the difference between the floating potential of the probe at the two points if the electron temperature is constant. Any thermionic emission from the probe caused by beam heating is limited by the beam plasma density and hence the alteration in floating potential is independent of position. However, the plasma potential must be corrected for the effects of charge exchange neutralization.

The Langmuir probes shown in Fig.6 have been constructed of tantalum and alumina to withstand the beam heating up to beam energies of the order of 25 keV. They have been used to measure the dependence of the potential on the main beam parameters, in particular the gas density, beam radius and beam energy.

In figs. 7 and 8, the well potential is shown as a function of gas density for helium beams in helium, hydrogen and argon. These curves show that the potential decreases with increasing gas pressure and then remains constant at high pressures. The experimental data and theory agree well over the entire pressure range for each gas.

The change in the scaling of the potential with pressure occurs when the slow ion density exceeds the beam ion density so that the electron density has to neutralise the space charge of the slow ions instead of the beam. In fig. 9, the theoretical peak slow ion and electron densities are plotted as a function of pressure for the experimental beam used to obtain the data shown in fig. 7. It can be seen that n_{io} increases almost linearly with pressure whereas n_{eo} only rises slowly at low pressure and then more rapidly as n_{io} becomes greater than n_{bo}.

The limiting value of ϕ_w at high pressures scales as $[\sigma m_i^{\frac{1}{2}}/\sigma_i]^{\frac{1}{2}}$ which depends strongly on the atomic species of the neutralizing gas. This scaling can be used as an indirect test of the validity of the model by comparing the values obtained from the well potential with published data on the cross-sections. Using the data from fig. 7, the low limit for ϕ_w yields the following cross-section ratios, $\sigma_1\sigma_{i2}/\sigma_2\sigma_{i1}$, which are in fair agreement with published data, from references 16 and 17 where σ_1 and σ_2 are the sum of σ_i and σ_{io} for the two gases used to derive the ratio.

	Experimental Data	Published Data
He/Ar	5.2	5.1
He/H_2	6.9	7.9
H_2/Ar	0.76	0.64

The variation of the well potential with beam energy is shown in fig. 10. The theoretical curve includes the effects of the variation of the cross-sections with beam energy and agrees fairly closely with experiment.

The dependence of the potential well on beam current and beam radius is difficult to analyse experimentally because the beam divergence is a function of the beam current for a given extraction system at constant beam energy and pressure. However if the beam potential is measured at various points along the axis of a diverging beam it is possible to derive the potential at several different radii and this is shown in Fig.11. The beam radius is found from the beam divergence, measured using a set of calorimeters. The experimental dependence of the beam potential is virtually $r^{-1.6}$ and agrees well with theory.

6.2 Energy Analysis

The main method of operation of this probe is to use the grid as a filter so that only ions or electrons are allowed to reach the collector. The energy of these particles which pass through the grid can then be analysed by biasing the collector and measuring the collected current.

The electron temperature, T, may be easily found with this probe by plotting current-voltage characteristic on log-linear axes and measuring the slope. In fig. 12 the dependence of T on gas density is shown which has a prenounced minimum at around pressures of 10^{-3} torr and agrees well with theory. It can be seen in fig. 9 that the minimum value of T coincides with the pressure where n_{io} equals n_{bo}.

The ion current-voltage characteristic can be used to obtain an estimate for ϕ_w and β^2. However repulsion of the electrons from the grid creates a space charge potential which causes an offset between the collector potential and the ion energy. The shape of the characteristic and noting the potential at which the current saturates, enables an approximate value for ϕ_w and β^2 to be derived.

The dependence of ϕ_w with gas pressure is shown in fig. 7 where it agrees closely with the Langmuir probe data. In fig. 13 the dependence of β with gas density is shown. The value of β derived from the numerical solution of Poisson's equation is also shown on the same graph and fairly good agreement is obtained.

The very slow change of β with gas density is caused by change in the value of n_{eo}/n_{bo} from unity which can be seen in Fig.9. This would affect the value of β^2 derived in equation 24.

6.3 Beam Divergence

Only a very limited description of the beam envelope is presented here and a more detailed discussion of the effects of space charge neutralization on the beam envelope will be published later. The radial electric field derived in Section 4 can be combined with the beam envelope equation developed by Kapchinskij and Vladimirskij[18] to provide a complete description of the beam envelope and beam divergence. The form of the equation shows that the divergence angle is approximately proportional to the radial electric field. Hence it is possible to compare the relative divergences of a vacuum (or unneutralized) beam and a neutralized beam by comparing the scalings of the electric field. These are respectively:

$$\text{Vacuum beam} \qquad E \propto n_{bo} r_o$$

$$\text{Neutralized beam} \qquad E \propto \left(\frac{n_{bo}}{n} \right)^{2/3} \cdot \frac{1}{r_o}$$

which shows that the field of the neutralized beam decreases with increasing beam radius unlike the vacuum beam. Hence it is expected that the divergence will decrease with increasing beam radius at constant beam density. This leads to the surprising conclusion that large diameter high current ion beams have lower divergences than small diameter low current beams.

This conclusion has been tested experimentally using the apparatus described in Section 6. The plasma source was a reflex arc source operated in low magnetic field to produce a quiescent plasma. The divergence was measured using a set of calorimeters which eliminates any uncertainties caused by electron collection or emission when electrical measurements of divergence are made. The results are shown in Fig.14 and it can be seen that the divergence of a helium beam decreases with increasing extraction aperture radius. The perveance density (electron perveance) and gas density were approximately constant over the entire series of measurements being respectively 5.3×10^{-7} AV$^{-3/2}$cm^{-2} and 6×10^{-4} torr.

The scaling of the lowest curve with beam energy suggests that the 6 mm radius beam has attained the fundamental emittance limit so that the space charge forces are less powerful than the finite ion temperature, T_{ib}, which causes a divergence of $(T_{ib}/V_b)^{\frac{1}{2}}$ radians and results in an intense ion beam with a normalized brightness of 3.10^{12} mA/cm^2/ster.

7. CONCLUSIONS

A theoretical model for the behaviour of the beam plasma in intense ion beams including both the particle and energy balance has been developed, the results of which are in good agreement with experiment. The behaviour of the beam plasma has suggested methods by which the plasma potential can be reduced, either by increasing the gas density or by increasing the beam diameter.

This last method is extremely useful since the residual divergence of the ion beam can be reduced by increasing the perveance. The large 6 mm diameter beam is virtually space charge free and of very high brightness. It can be easily utilized in C.T.R. work for diagnostics or neutral injection.

ACKNOWLEDGEMENTS

The author would like to thank Drs E Thompson, T S Green and J C Cordey for many useful discussions and also Mr L A J Verra for his aid on the numerical solution to the problem.

REFERENCES

[1] Cordey, J G , Proc. on Theoretic and Experimental Aspects of Heating Toroidal Plasmas 2 pp.107-115, Grenoble, 1976.

[2] Cordey, J G and Core, W G F., Nuclear Fusion 15 pp.710-712, 1975.

[3] Kulsrad R M and Jassby, D L., Nature 259 pp.541-544. 1976.

[4] Gabovich, M D, Katsubo, L P and Solovhenko, I A, Sov. J. Plasma Phys., 1, pp.162-164, 1975.

[5] Hamilton, G. Private communication.

[6] Dunn, D A and Self, S A, J. App. Phys., 35, pp.113-122, 1964.

[7] Green, T S. To be published.

[8] Spitzer, L, Physics of Fully Ionized Gases, Interscience Publications, New York, 1962.

[9] Cordey, J G, Phys. Fluids, 14, pp. 1407-1410, 1971.

[10] Rosenbluth, M N, MacDonald, W M and Judd, D L, Phys. Rev. 107, pp.1-6, 1957.

[11] Rudd, M E and Jorgensen, T. Jr., Phys. Rev., 131, pp.666-675, 1963.

[12] Harrison, E R and Thompson, W B., Proc. Phys. Soc., 74, pp.145-162, 1959.

[13] Holmes, A J T and Thompson, E. To be published.

[14] Thompson, E., Conf. Ion Sources and Beams, II7, Berkeley, 1974.

[15] Gryzinski, M., Phys. Rev., 115, pp.374-383, 1959.

[16] Solovev, E S, Ilin, R N, Oparin, V and Fedorenko, N., Sov. Phys. J.E.T.P. 18, pp.342-345, 1964.

[17] Allison, S K., Rev. Mod. Phys., 30, pp.1137-68, 1958.

[18] Kapchinskij, I. and Vladimirskij, V. High Energy Accel. Conf., CERN, p.274, 1959.

APPENDIX I

In section 3.1 it was assumed that the potential could be represented by a series of the form:

$$-\phi(r) = \phi_o \frac{r^m}{r_o^m} + \phi_1 \frac{r^{m+1}}{r_o^{m+1}} + \phi_2 \frac{r^{m+2}}{r_o^{m+2}} + \ldots \qquad (A1)$$

providing $\phi(0) = 0$. Here it will be shown that the index, m, must be necessarily two in order to have a physically meaningful value for the slow ion density on axis.

As before, attention is restricted to a small region around the axis so that only the first term in equation A1 is dominant. The integral in equation 2 becomes on simplification:-

$$n_i(a) = \frac{n_{bo}\sigma n v_b r_o}{(2e/m_i)^{\frac{1}{2}}\,(-\phi_o)^{\frac{1}{2}}} \cdot \int_o^1 \frac{u^{-(m-2)/m}}{m(1-u)^{\frac{1}{2}}}\,du$$

where $u = r^m/a^m$. This integral may be solved to give:

$$n_i(a) = \frac{n_{bo}\sigma n v_b r_o^{1-m/2}}{(2e/m_i)^{\frac{1}{2}}\,\phi_o^{\frac{1}{2}}} \cdot \sqrt{\pi}\,\frac{\Gamma(1 - (m-2)/m)}{\Gamma(3/2 - (m-2)/m)} \qquad (A2)$$

It can be seen that if m is greater than two when a tends to zero, the axial ion density tends to infinity. If m is less than two, the axial ion density tends to zero. Both of these solutions are non-physical hence m must be exactly equal to two to yield a non-zero finite value for n_{io} and this has been assumed in equation 3. Thus when m = 2

$$n_{io} = n_{bo}\sigma n v_b r_o/(2e/m_i)^{\frac{1}{2}}\,\phi_o^{\frac{1}{2}}$$

APPENDIX II

The Distribution of Newly Created Electrons

When electrons have been created by ionization, the beam ions give them a small amount of kinetic energy. A theoretical model by Gryzinski [15] has determined this velocity distribution which is proportional to the beam velocity, v_b. Experimental work by Rudd and Jorgensen [14] has confirmed this velocity distribution. It is assumed here that this velocity is isotropic and hence the electrons will have an angular momentum of the order of ρw about the beam axis where ρ is the radius at which they were created. This forces the electrons to have elliptic orbits around the beam axis if the potential well is parabolic. The equations of motion for the electrons are:

$$\frac{m_e v_r^2}{2} + \frac{m_e v_\theta^2}{2} = e\Delta\phi + \frac{m_e w^2}{2}$$

and

$$r v_\theta = \rho w$$

where v_r and v_θ are the radial and azimuthal velocities and w is the initial velocity of the electron. If the well is assumed to be parabolic in the axial region then

$$\Delta\phi = \frac{\phi_o}{r_o^2}(\rho^2 - r^2)$$

Hence:

$$v_r^2 = \frac{2e\phi_o}{m_e r_o^2}(\rho^2 - r^2) + w^2 - v^2$$

$$= (\rho^2 - r^2) \cdot \left(\frac{2e\phi_o}{m_e r_o^2} - \frac{w^2}{r^2}\right)$$

The elliptic orbit intersects any given radius r, which is less than ρ, four times during a single orbit whose period τ is equal to $2\,(m_e r_o^2/2e\phi_o)^{\frac{1}{2}}$. Hence:

$$\frac{dN_e}{dt} = \int_r^\infty nn_b \sigma_i v_b \frac{4}{2\pi r v_r \tau} \cdot 2\pi\rho d\rho$$

$$= \int_r^\infty nn_{bo} \exp - \frac{\rho^2}{r_o^2} \sigma_i v_b \cdot \frac{4(2e\phi_o)^{\frac{1}{2}} \cdot \rho d\rho}{2\pi r(\rho^2 - r^2)^{\frac{1}{2}} (m_e r_o^2)^{\frac{1}{2}}}$$

$$x \int_o^{w_m} \frac{f(w)dw}{(2e\phi_o/m_e r_o^2 - w^2/r^2)^{\frac{1}{2}}}$$

where f(w) is the distribution function of the initial velocities and w_m^2 equals $2er^2\phi_o/m_e r_o^2$. This function may be approximated by:-

$$f(w) \simeq \frac{2}{v_b^2} \exp - w^2/v_b^2 \cdot wdw.$$

This expression gives moderate agreement with the results obtained by Rudd and Jorgensen except at low values of w.

If the above two equations are combined and $2e\phi_o r^2/m_e r_o^2 v_b$ is less than unity which applies for $r < r_o$, then

$$\frac{dN_e}{dt} = \frac{4nn_b \sigma_i v_b r}{\pi^{\frac{1}{2}} r_o} \cdot \frac{e\phi_o}{m_e v_b^2}$$

The net effect of the finite velocity of the electrons is to transfer the electrons from the centre to edge as their angular momentum prevents most of these electrons from reaching the centre of the beam. The above relation breaks down at radii greater than r_o but as the most effective energy absorption occurs at the centre where the containment time is longest, this effect is unimportant.

FIGURE CAPTIONS

Fig. 1 The dependence of the electron distribution function on the potential well depth ϕ_w

Fig. 2 Particle and energy transfer between the particle distributions. The total energy and particle content of each distribution is constant.

Fig. 3 The detailed shape of the electron distribution including the effects of newly created electrons.

Fig. 4 The shape of the potential well and particle profiles at low pressure; beam energy 20 keV He^+, pressure 1.25 10^{-4} torr, current 17.6 mA, radius 5 mm.

Fig. 5 The shape of the potential well and particle profiles at high pressure; beam energy 20 keV He^+, pressure 2.10^{-3} torr, current 17.6 mA, radius 5 mm.

Fig. 6 The beam line.

Fig. 7 The beam potential, ϕ_w, as a function of gas pressure, beam energy 20 keV He^+, beam radius 5 mm, current 17.6 mA.

Fig. 8 The beam potential, ϕ_w, as a function of gas pressure, beam energy 20 keV He^+, beam radius 1.4 mm, current 10 mA.

Fig. 9 Ratio of electron or ion density to axial beam density as a function of pressure. Beam energy 20 keV He^+, current 17.6 mA, radius 5 mm.

Fig. 10 Beam potential, ϕ_w, as a function of beam energy, current 17.6 mA, beam radius 5 mm, pressure 7.10^{-5} torr.

Fig. 11 Beam potential, ϕ_w, as a function of beam radius, current 17.6 mA, beam energy 20 keV He^+, pressure 7.10^{-5} torr.

Fig. 12 Electron temperature as a function of pressure, beam energy 20 keV He^+, beam radius 5 mm, current 17.6 mA.

Fig. 13 Radius ratio, β, as a function of pressure; beam energy 20 keV He^+, current 17.6 mA, radius 5 mm.

Fig. 14 Beam divergence as a function of beam energy and beam radius for an He^+ beam.

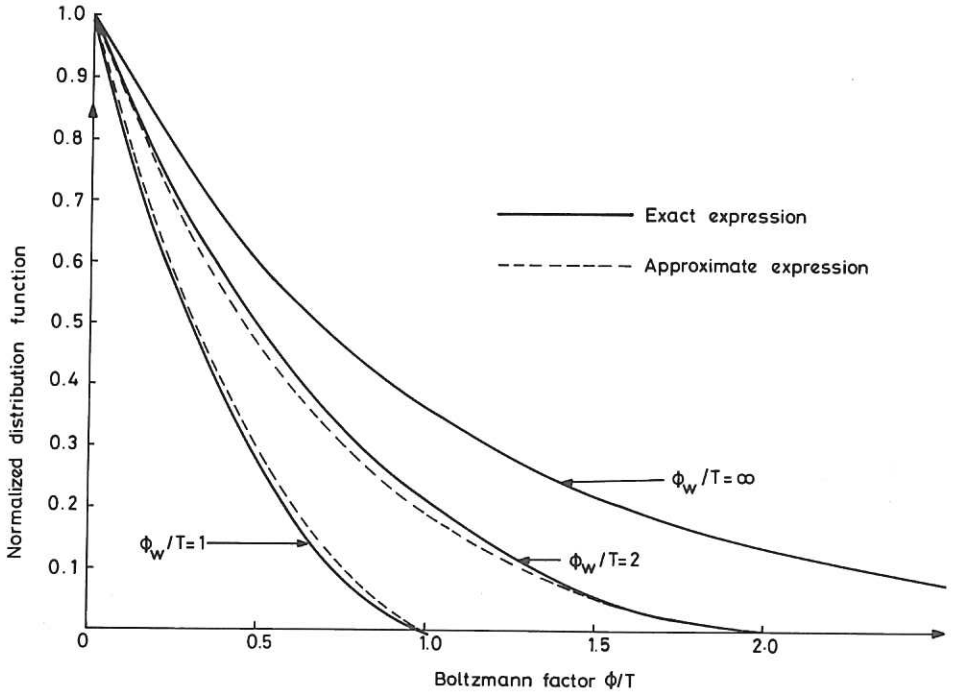

Fig.1 The dependence of the electron distribution function on the potential well depth ϕ_w.

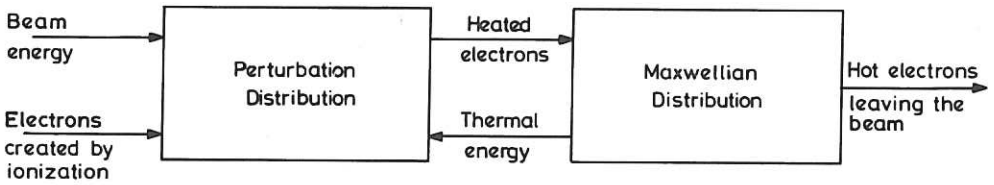

Fig.2 Particle and energy transfer between the particle distributions. The total energy and particle content of each distribution is constant.

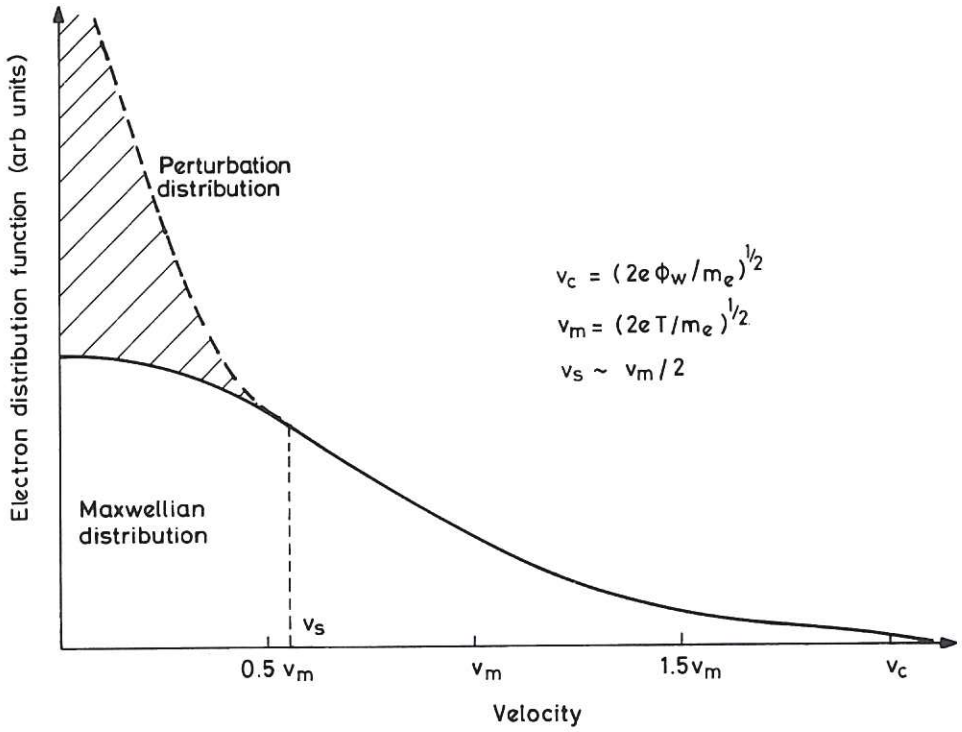

Fig.3 The detailed shape of the electron distribution including the effects of newly created electrons.

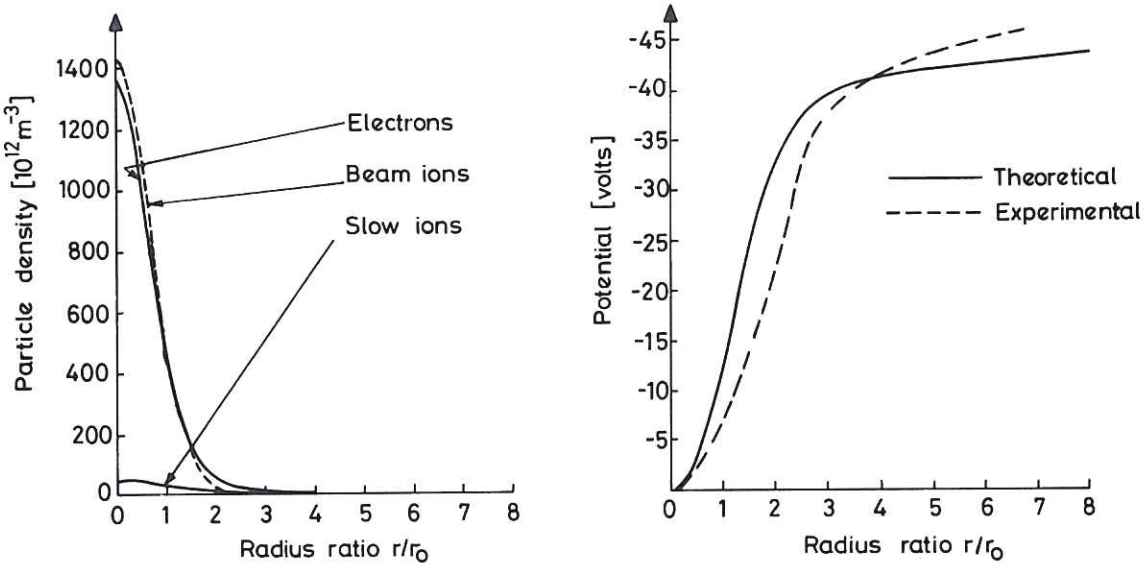

Fig.4 The shape of the potential well and particle profiles at low pressure; beam energy 20keV He^+, pressure 1·25 10^{-4} torr, current 17·6mA, radius 5mm.

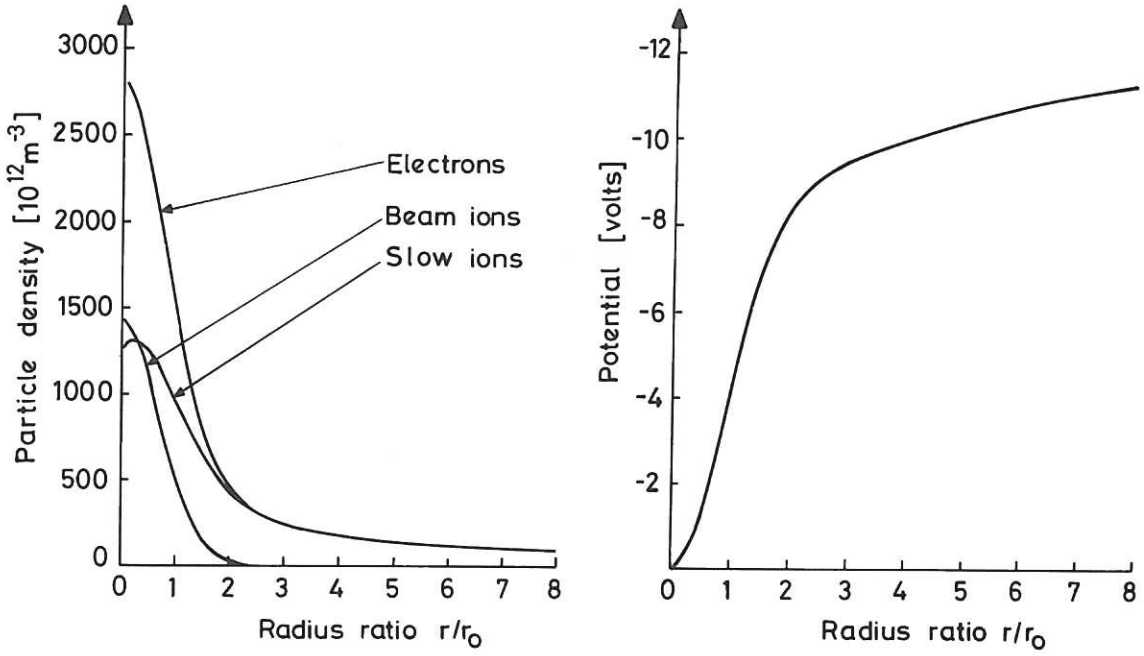

Fig.5 The shape of the potential well and particle profiles at high pressure; beam energy 20keV He^+, pressure $2 \cdot 10^{-3}$ torr, current 17·6mA, radius 5mm.

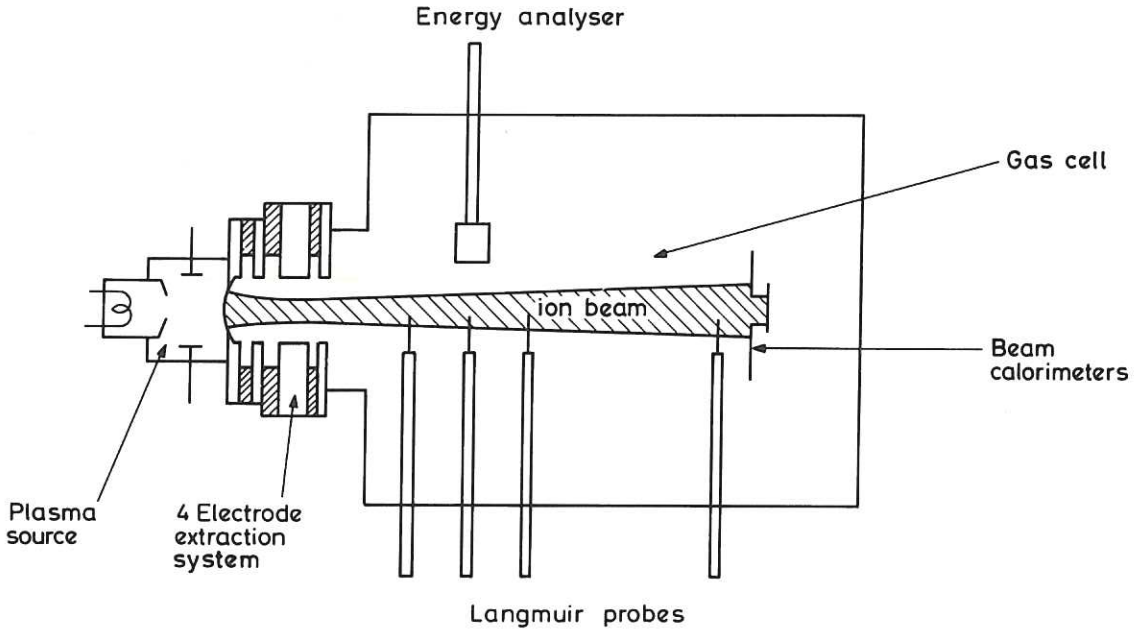

Fig.6 The beam line.

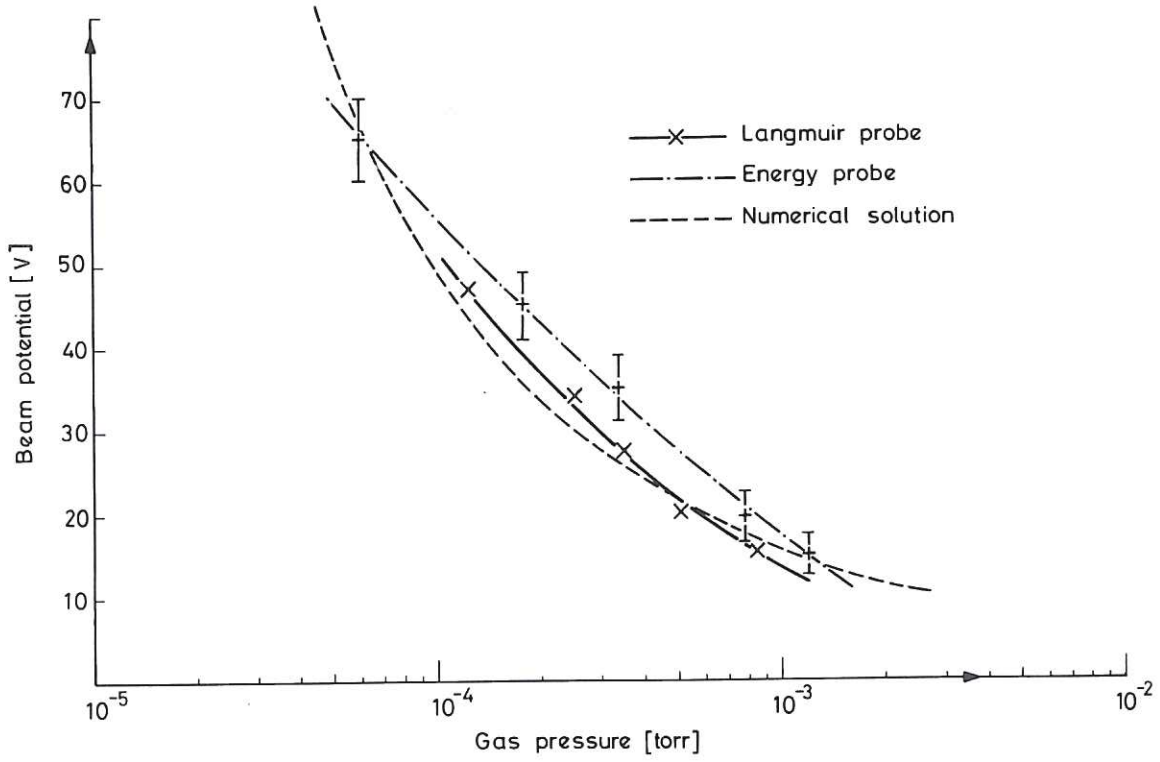

Fig.7 The beam potential, ϕ_W, as a function of gas pressure, beam energy 20keV He^+, beam radius 5 mm, current 17·6 mA.

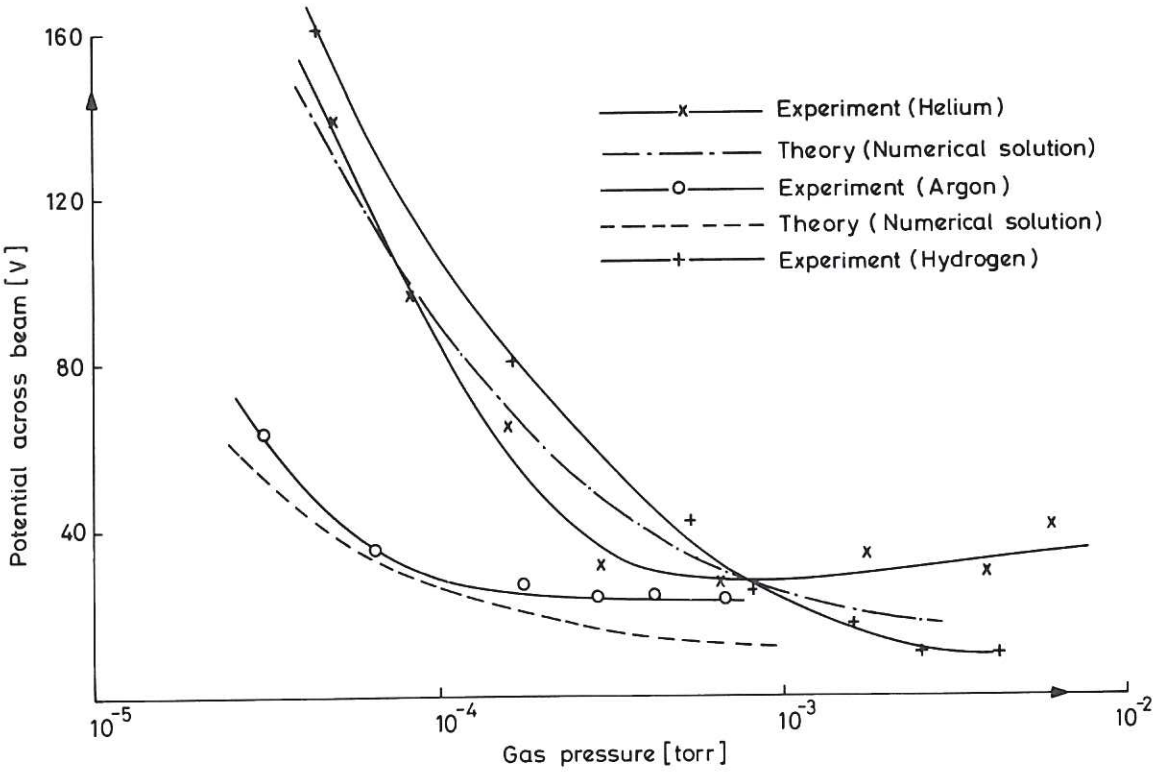

Fig.8 The beam potential, ϕ_W, as a function of gas pressure, beam energy 20keV He^+, beam radius 1·4 mm, current 10 mA.

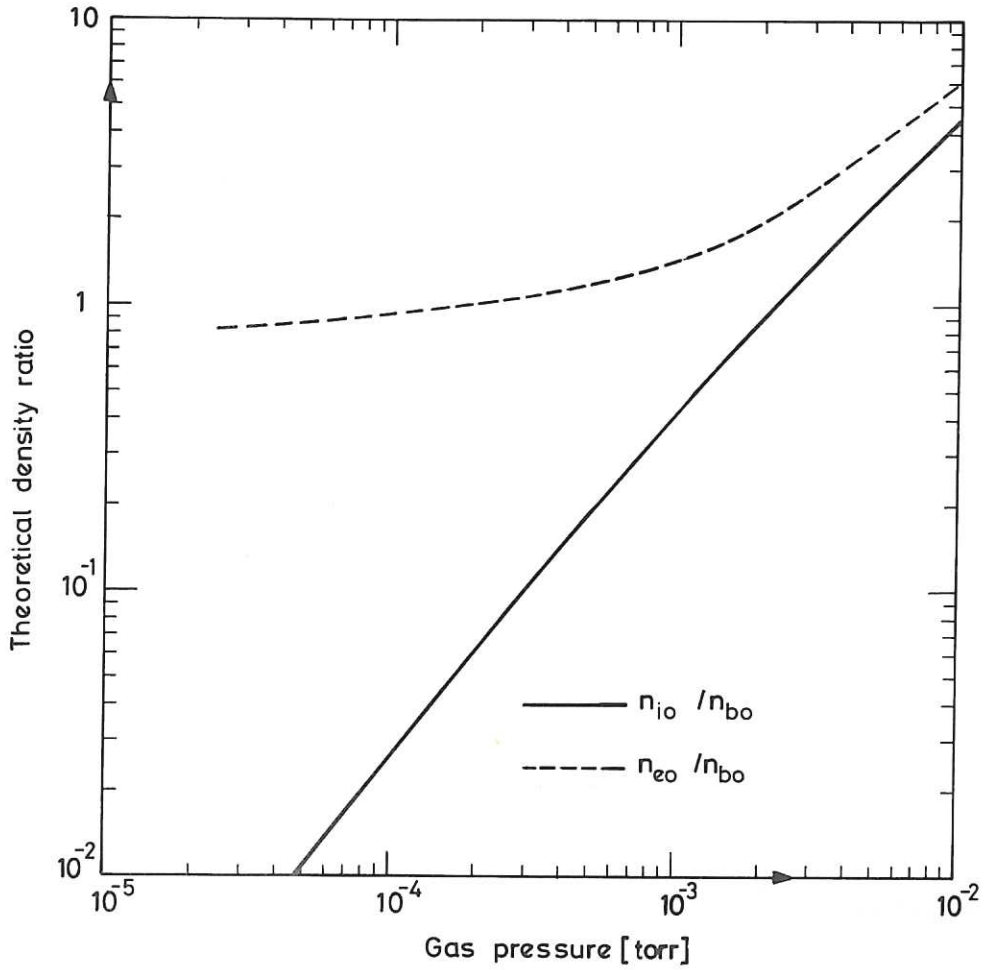

Fig.9 Ratio of electron or ion density to axial beam density as a function of pressure. Beam energy 20keV He^+, current 17·6mA, radius 5mm.

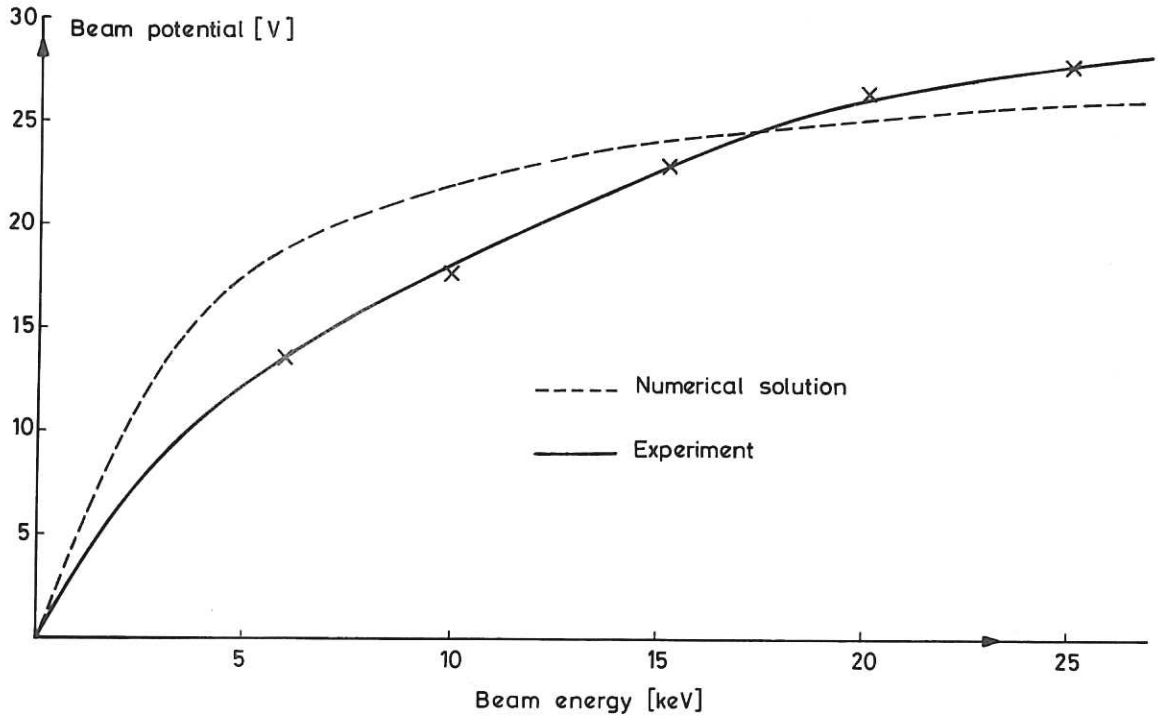

Fig.10 Beam potential, ϕ_w, as a function of beam energy, current 17·6mA, beam radius 5mm, pressure $7 \cdot 10^{-5}$ torr.

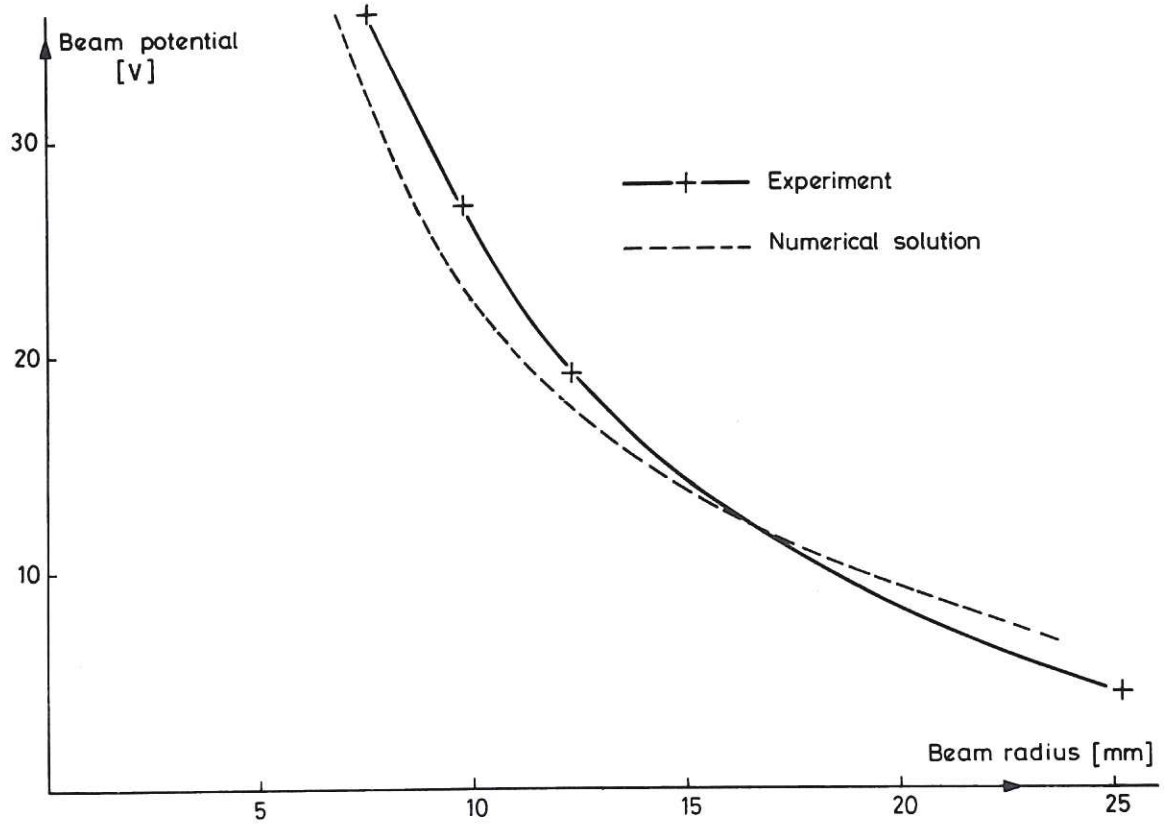

Fig.11 Beam potential, ϕ_W, as a function of beam radius, current 17·6mA, beam energy 20keV He^+, pressure $7 \cdot 10^{-5}$ torr.

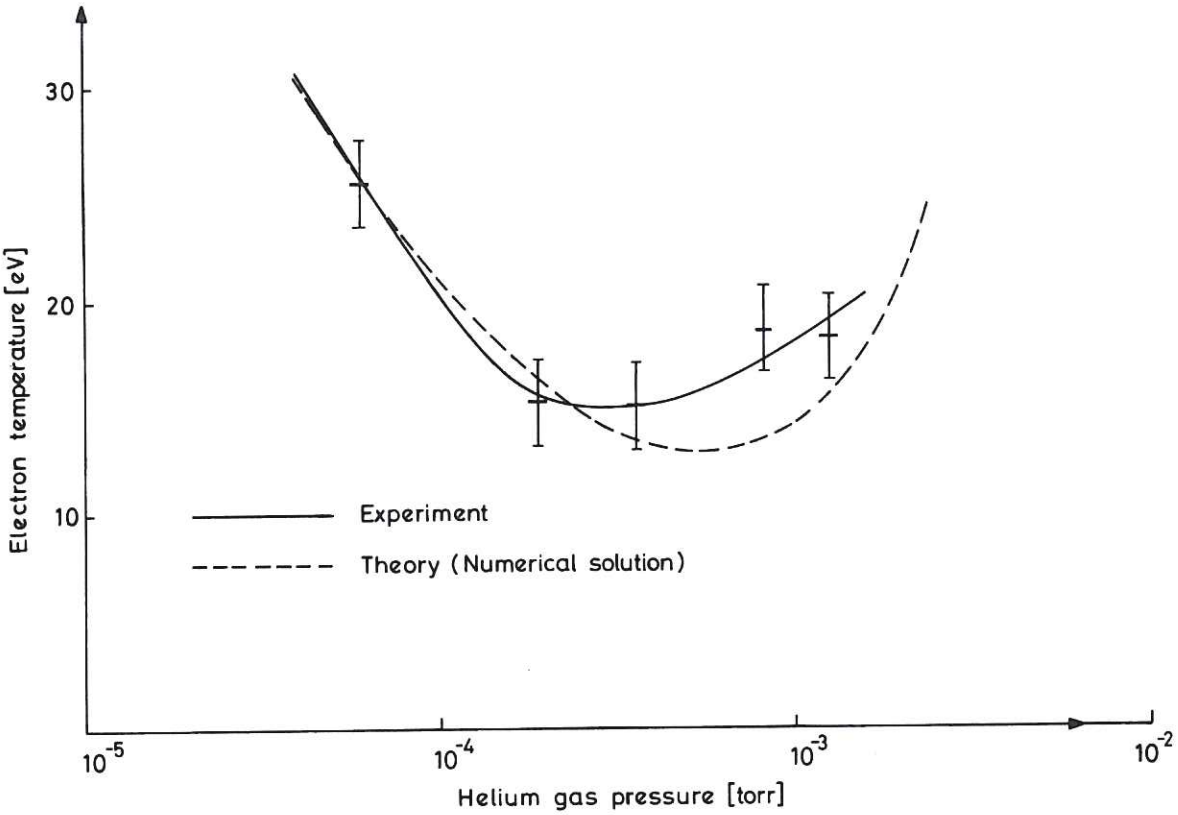

Fig.12 Electron temperature as a function of pressure, beam energy 20keV He^+, beam radius 5mm, current 17·6mA.

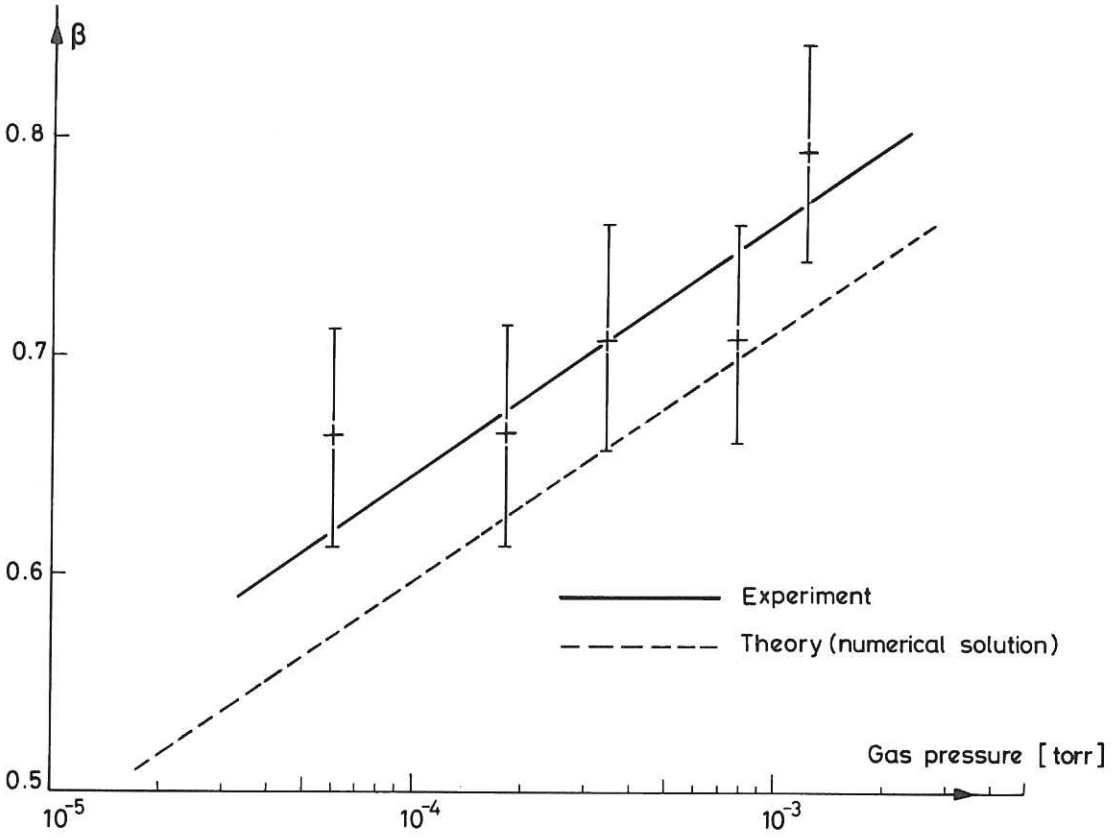

Fig.13 Radius ratio, β, as a function of pressure; beam energy 20keV He^+, current 17·6mA, radius 5mm.

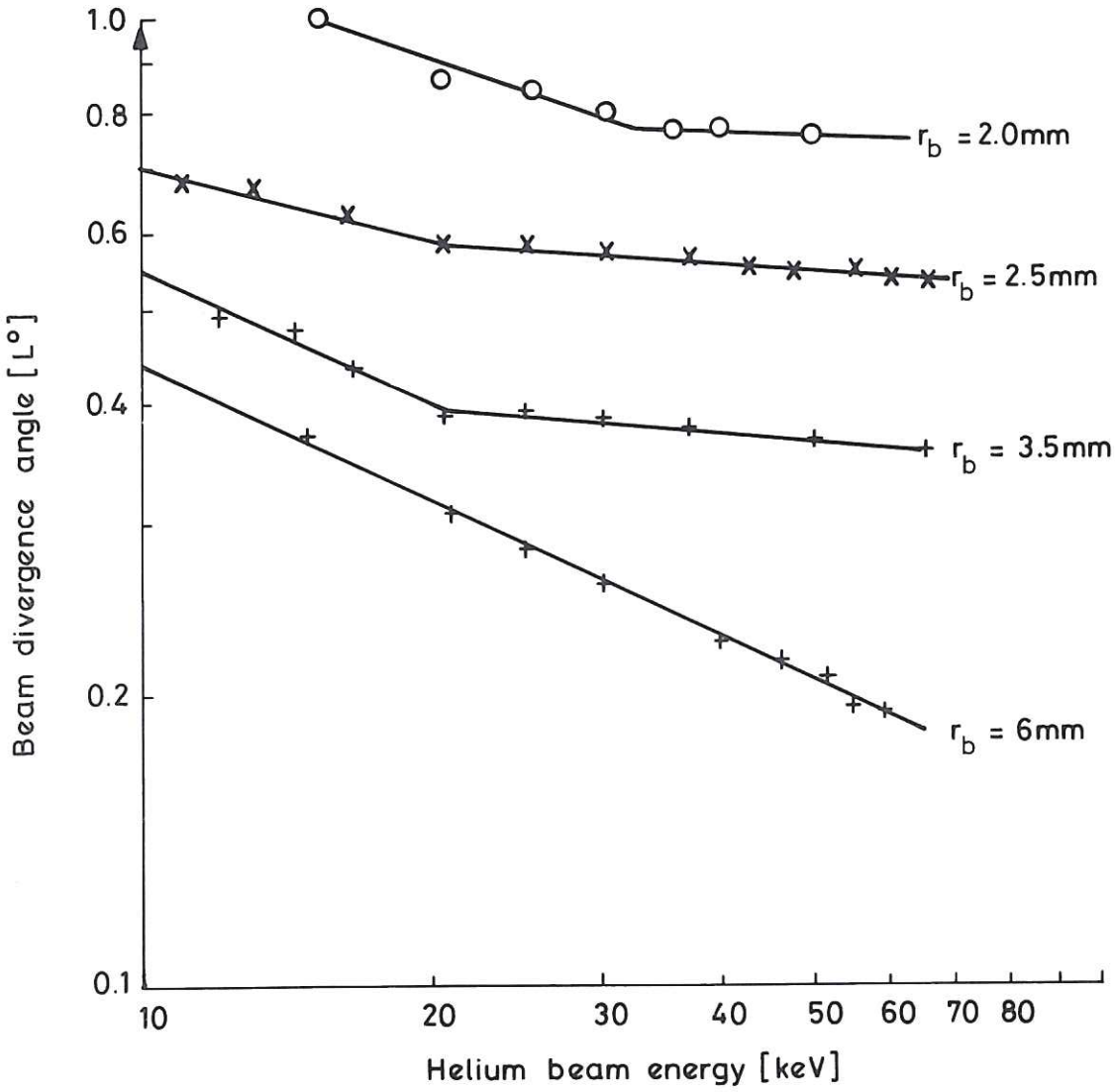

Fig.14 Beam divergence as a function of beam energy and beam radius for an He^+ beam.